Tasmanian Geological Survey
Record 2013/02
Geoscience Australia
Record 2013/22

New SHRIMP U-Pb zircon ages from Tasmania

by N. Kositcin and J. L. Everard

Mineral Resources Tasmania
Department of Infrastructure, Energy and Resources

Tasmania
Explore the possibilities

New SHRIMP U–Pb zircon ages from Tasmania

July 2012–June 2013

GEOSCIENCE AUSTRALIA
RECORD 2013/22

MINERAL RESOURCES TASMANIA
TASMANIAN GEOLOGICAL SURVEY RECORD 2013/02

N. Kositcin[1] and J.L. Everard[2]

Australian Government
Geoscience Australia

Mineral Resources Tasmania
Department of Infrastructure, Energy and Resources

1. Minerals and Natural Hazards Division, Geoscience Australia, GPO Box 378, Canberra ACT 2601
2. Mineral Resources Tasmania, PO Box 56, Rosny Park TAS 7018

Department of Resources, Energy and Tourism

Minister for Resources and Energy: The Hon Gary Gray AO MP
Secretary: Mr Blair Comley, PSM

Geoscience Australia
Chief Executive Officer: Dr Chris Pigram
This paper is published with the permission of the CEO, Geoscience Australia

Department of Infrastructure, Energy and Resources (Tasmania)
Minister for Energy and Resources: Mr Bryan Green MHA
Chief Executive/Secretary: Mr Norm McIlfatrick

Mineral Resources Tasmania
Executive Director: Kim Creak

ISSN 2201-702X (PDF)

ISBN 978-1-922201-53-9 (PDF)

GeoCat 76210

Bibliographic reference: Kositcin, N. & Everard, J.L. 2013. *New SHRIMP U–Pb zircon ages from Tasmania: July 2012–June 2013*. Geoscience Australia Record 2013/22, Tasmanian Geological Survey Record 2013/02. Geoscience Australia: Canberra.

Contents

Executive Summary

This Record contains new zircon U–Pb geochronological data obtained via Sensitive High-Resolution Ion Micro Probe (SHRIMP) from six samples of granitic rocks: five from the Eastern Tasmania Terrane and one from the Western Tasmania Terrane. These data were obtained during the reporting period July 2012–June 2013, under the auspices of the collaborative Geochronology Project between the Mineral Resources Tasmania (MRT) and Geoscience Australia (GA).

The primary objective of this study is to refine the regional chronology of mid-Paleozoic felsic plutonism in Tasmania established by Black et al. (2005). In some cases, the samples were chosen because of economic importance, or to help resolve regional problems. The results are summarised in Table 1.1 and below.

Eastern Tasmania Terrane

The oldest two samples analysed are associated with the Scottsdale Batholith of northeastern Tasmania. The chemically unfractionated I-type Lisle Granodiorite intrudes Ordovician to Lower Devonian Mathinna Supergroup sedimentary rocks about 3 km south of Lisle, is either coeval or slightly older than local gold mineralisation, and yielded a magmatic crystallisation age of 393.3 ± 2.0 Ma (all uncertainties are quoted at the 95% confidence level). The fractionated I-type Mount Stronach Granite is the most felsic unit of the Scottsdale Batholith, is associated with minor molybdenum mineralisation at Mount Stronach about 6 km east-northeast of Scottsdale, and yielded a magmatic crystallisation age of 392.2 ± 1.9 Ma. The two new dates are indistinguishable from each other, and are also within uncertainty of the 390.4 ± 2.2 Ma Diddleum Granodiorite (Black et al., 2005), which is chemically similar to the Lisle Granodiorite. However, both of the new dates are distinguishably older than two other Scottsdale Batholith plutons: the 387.8 ± 2.3 Ma Hogarth Road Granite and the 385.9 ± 2.8 Ma Tombstone Creek Granite (Black et al., 2005).

Two more samples were obtained from the Gipps Creek Granite and the Royal George Granite, which were formerly grouped with the 376.7 ± 2.7 Ma I-type Henbury Granite (Black et al., 2005) as the Ben Lomond Batholith. The strongly fractionated S-type Gipps Creek Granite is associated with significant tin-tungsten mineralisation about 6 km west-southwest of Rossarden, and yielded a magmatic crystallisation age of 381.7 ± 2.2 Ma, which indicates that dates of 365 Ma (Rb–Sr whole-rock–feldspar isochron) and 352 Ma (K–Ar muscovite) determined by McDougall and Leggo (1965) have been at least partially reset. The S-type Royal George Granite was collected about 3 km south-southwest of Royal George, where it is associated with significant greisen-style tin mineralisation. It yielded a SHRIMP U–Pb magmatic crystallisation age of 377.1 ± 1.8 Ma. The Gipps Creek Granite is distinguishably older than both the Henbury Granite and the Royal George Granite, although the latter pair are indistinguishable from each other. In addition, the Royal George Granite is indistinguishable in age from the chemically similar 377.8 ± 2.4 Ma Lottah Granite of the Blue Tier Batholith to the north (Black et al., 2005).

The fifth sample was obtained from The Hazards Granite, one of several fractionated I-type granites of the Freycinet Peninsula, which collectively constitute the Freycinet Suite in northeastern Tasmania. It

yielded a magmatic crystallisation age of 379.3 ± 1.9 Ma, which suggests that dates of 375 Ma (Rb–Sr biotite), 350 Ma (K–Ar biotite) and 345 Ma (Rb–Sr whole-rock–feldspar isochron) previously determined on granites of the Freycinet Suite (McDougall and Leggo, 1965) have been at least partially reset. The age of The Hazards Granite is indistinguishable from that of the 381.4 ± 2.7 Ma Bicheno Granite (Black et al., 2005) to the north.

Western Tasmania Terrane

The Meredith Granite is a fractionated I-type alkali feldspar granite associated with significant tin mineralisation, and is the largest exposed granite body in western Tasmania. The unit was sampled in drillcore some 16 km north-northwest of Renison Bell, northwestern Tasmania, and yielded a magmatic crystallisation age of 372.2 ± 1.9 Ma. This age is indistinguishable from the SHRIMP U–Pb age of the Wombat Flat Granite (373.2 ± 1.9 Ma, Black et al., 2005), which is assigned to the same suite (McClenaghan, 2006).

1. Introduction

This Record contains new zircon U–Pb geochronological data obtained via Sensitive High-Resolution Ion Micro Probe (SHRIMP) from six samples of granitic rocks of the Eastern and Western Tasmania Terranes. The samples are derived from Devonian granites in order to provide a more robust chronological record of mid-Paleozoic felsic magmatism in Tasmania. These data were obtained during the reporting period July 2012–June 2013, under the auspices of the collaborative Geochronology Project between the Mineral Resources Tasmania (MRT) and Geoscience Australia (GA), which is part of the National Geoscience Accord.

Devonian–Carboniferous granites, exposed over about 6% of the Tasmanian landmass, consist of more than 80 geochemically and mineralogically distinct plutons or spatially separate bodies (named and classified by Everard (2005)), which intrude lithologically diverse Proterozoic and Early Paleozoic rocks. The granites are an important source of the mineral wealth of Tasmania, as fluids derived from them were responsible for major Sn, W and base-metal deposits within, adjacent to, and more distal to the intrusions. The accurate determination of their age is therefore vitally important for any comprehensive understanding of the geological evolution of Tasmania and its ore deposits.

Five samples were analysed from the Eastern Tasmanian Terrane — three granites from LAUNCESTON (1:250 000 map sheet) two from OATLANDS, and one sample from the Western Tasmanian Terrane (BURNIE) (Figures 1.1 and 1.2).

Dating of Tasmanian granites began with the extensive K–Ar and Rb–Sr study of McDougall and Leggo (1965), which revealed that the Devonian to Carboniferous plutons in east Tasmania tended to yield older ages than those in the west. Significant later studies of those rocks include those of Brooks (1966), Brooks and Compston (1965) and Sawka et al. (1990) in western Tasmania, and Cocker (1982), Turner et al. (1986) and Mackenzie et al. (1988) in eastern Tasmania.

More recently, Black et al. (2005, 2010) provided SHRIMP U–Pb results for some 25 granites throughout Tasmania. Their data show: a) Devonian–Carboniferous magmatism in both eastern and western Tasmania was spread over a 50 million year period (from 400 Ma to 350 Ma), b) there is a westward younging of granites regionally across Tasmania, c) there is a significant compositional trend towards felsic, fractionated I-type and S-type granite and monzogranite with decreasing age, and d) many previously reported mineral and whole rock K–Ar and Rb–Sr ages have been isotopically reset.

This Record documents detailed results for each sample individually, encompassing sample location, geological context, zircon descriptions, an evaluation of the relevant analytical data (including chemistry), and a brief geochronological interpretation. The results are summarised in Table 1.1 and Figure 1.3, and are also available via GA's Geochron Delivery system (accessible at http://www.ga.gov.au/geochron-sapub-web/geochronology/shrimp/search.htm). A comprehensive description of sample acquisition and processing procedures, preparation and analysis of SHRIMP mounts, and data reduction and presentation methods are included in the Appendix, along with analytical session-specific details of the calibration data collected on the reference $^{238}U/^{206}Pb$ and $^{207}Pb/^{206}Pb$ zircons.

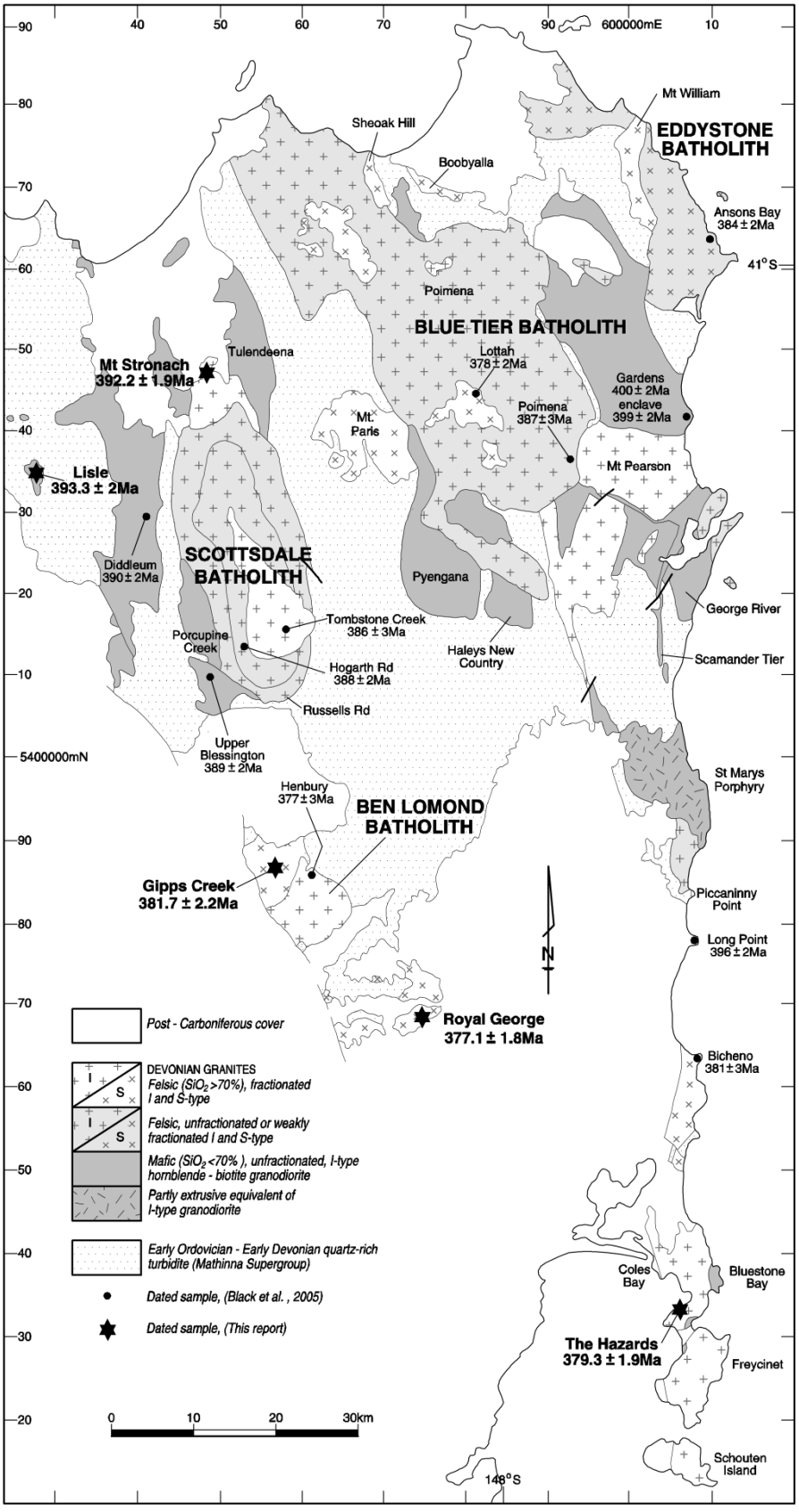

Figure 1.1 *Map of northeast Tasmania showing granite plutons, sample locations and newly determined emplacement ages; other plutons mentioned in the text are also labelled (modified after Black et al., 2005).*

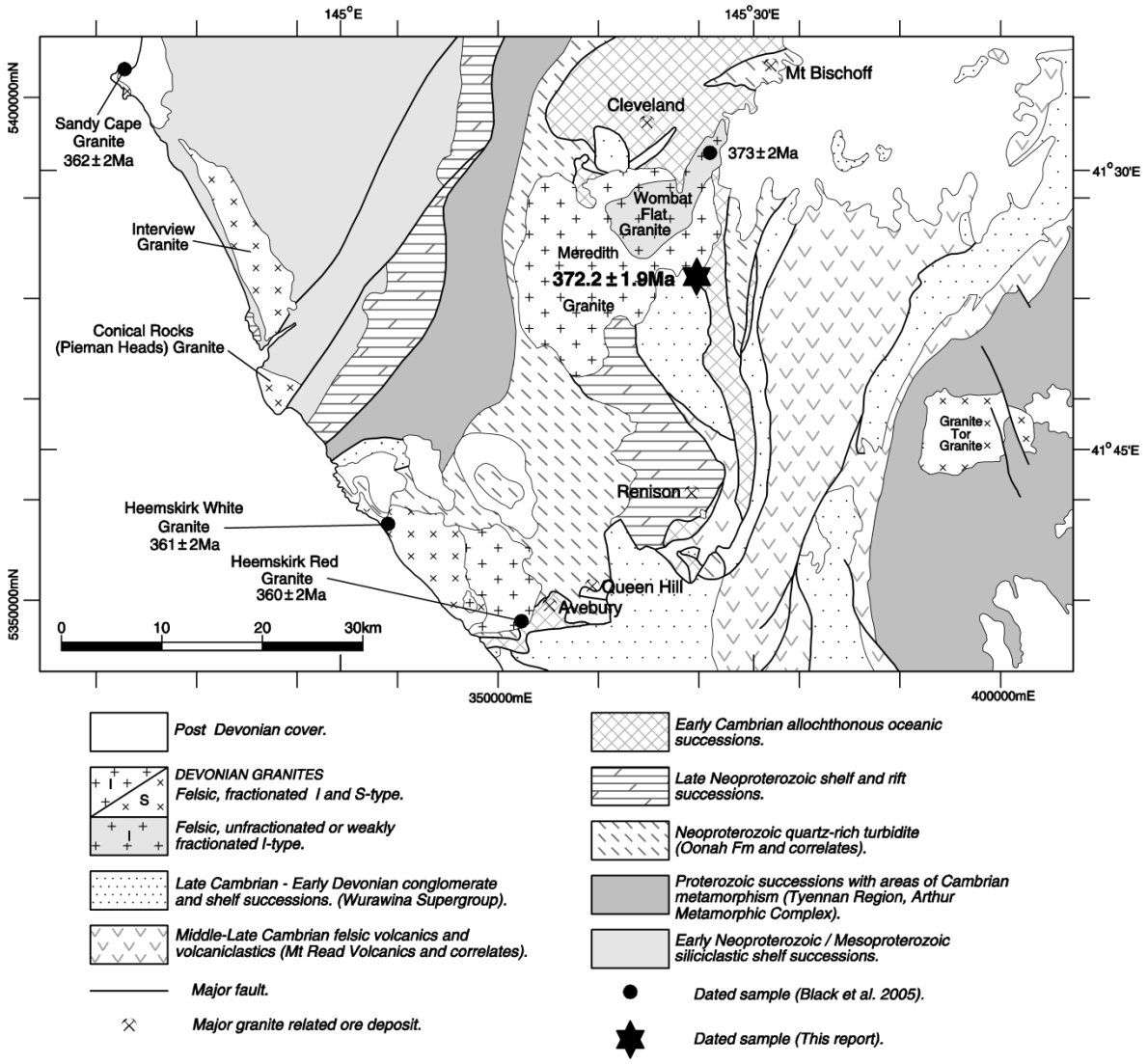

Figure 1.2 *Map of northwest Tasmania showing granite plutons, sample locations and newly determined emplacement ages; other plutons mentioned in the text are also labelled.*

Table 1.1 *Summary of sample identifiers, locations, stratigraphic units, and magmatic crystallisation ages for the MRT–GA Geochronology Project. n = number of analyses included in the weighted mean age.*

MRT Registration No.	GA SampleNo	Terrane	MGA94 Easting	MGA94 Northing	GDA94 Latitude	GDA94 Longitude	Unit Name	Magmatic $^{238}U/^{206}Pb$ Age (±95% confidence level)
R014555	2152726	Eastern Tasmania	527712	5432383	-41.2594870	147.3308153	Lisle Granodiorite	393.3 ± 2.0 Ma (n = 24)
R013228	2152729	Eastern Tasmania	548472	5446433	-41.1319531	147.5775115	Mount Stronach Granite	392.2 ± 1.9 Ma (n = 23)
R004491	2152728	Eastern Tasmania	572852	5367173	-41.8439815	147.8775332	Royal George Granite	377.1 ± 1.8 Ma (n = 24)
R004493	1951009	Eastern Tasmania	556532	5385183	-41.6831096	147.6792559	Gipps Creek Granite	381.7 ± 2.2 Ma (n = 25)
R004499	1950975	Eastern Tasmania	605442	5333133	-42.1468240	148.2761206	The Hazards Granite	379.3 ± 1.9 Ma (n = 23)
R017895	2153031	Western Tasmania	364258	5386705	-41.6598517	145.3696326	Meredith Granite	372.2 ± 1.9 Ma (n = 22)

Table 1.2 *Chemical analyses of the dated samples.*

Pluton	Mt Stronach	Royal George	Gipps Creek	Gipps Creek	Gipps Creek	The Hazards	The Hazards	The Hazards
Field No	NJ111	SG35	SG36	SG36	SG36	R004499	R004499	R004499
MRT Reg No	R013228	R004491	R004493	R004493	R004493	R004499	R004499	R004499
MRT Anal No	20080197	20010138	20010140			20010144		
GA Sample No				1951009	1951009		1950975	1950975
Majors Lab	MRT	MRT	MRT	GA		MRT	GA	
SiO_2 (wt%)	76.39	75.11	72.67	74.02		75.89	76.37	
TiO_2	0.06	0.06	0.17	0.17		0.07	0.07	
Al_2O_3	12.83	13.57	14.56	14.22		12.56	12.21	
Fe_2O_3	0.12	0.12	0.50	*2.13		0.35	*1.33	
FeO	0.80	1.09	1.47	nd		0.96	nd	
MnO	0.04	0.03	0.05	0.05		0.02	0.02	
MgO	0.09	0.18	0.30	0.19		0.13	0.03	
CaO	0.44	0.19	0.73	0.74		0.57	0.56	
Na_2O	3.59	3.05	3.54	3.56		3.42	3.44	
K_2O	4.56	4.97	4.68	4.79		4.98	5.02	
P_2O_5	0.00	0.16	0.13	0.11		0.03	0.01	
$H2O^+$	0.43	0.62	0.86			0.60		
$H2O^-$						0.60		
CO_2	0.00	0.01	0.09			0.01		
SO_3tot	0.03	0.02	0.03	0.03		0.03	0.03	
rest		0.10	0.13					
LOI				-0.12			0.80	
TOT	99.37	99.28	99.91	99.91		99.61	99.87	
LOI2	0.34	0.51	0.79			0.50		
Fe_2O_3/FeO	0.147	0.110	0.340			0.365		
FeOtot	0.91	1.20	1.92	1.92		1.28	1.20	
ASI	1.007	1.263	1.192	1.148		1.042	1.009	
trace method	XRF	XRF	XRF	XRF	ICPMS	XRF	XRF	ICPMS
trace lab	MRT	MRT	MRT	GA	GA	MRT	GA	GA
Be (ppm)					7.6			7.2
Sc	-9	-9	-9	6		-9	-1	
V	-5	13	13	7	7.2	9	1	1.2
Cr	8	-5	-5			-5		
Co	-8	-8	-8	1	1.5	-8	1	0.5
Ni	-5	6	5	4	11.9	5	3	6.7
Cu	7	-5	9	3	4.3	9	3	2.9
Zn	24	19	42	52	51.1	38	48	46.2

Pluton	Mt Stronach	Royal George	Gipps Creek	Gipps Creek	Gipps Creek	The Hazards	The Hazards	The Hazards
Ga	16	20	22	25.9	26.2	24	29.4	28.9
Ge					2.4			1.5
As	-20	-20	-20	-2	-0.5	-20	-2	-0.5
Rb	280	640	480	472.9	482.2	710	752.3	764.2
Sr	33	16	68	68.2	67.6	6	6.1	5.7
Y	37	39	45	44	39.3	180	183	172.2
Zr	63	60	100	111	106.1	120	127	135.4
Nb	11	15	19	21	21.1	29	31	31.5
Mo	-5	-5	-5	2	2.2	-5	2	2.1
Ag					-0.6			-0.6
Cd					0.1			0.0
Sn	-9	-9	12		15.8	17		34.6
Sb					-0.8			-0.8
Cs				28	27.1		21	20.2
Ba	110	45	210	183	197.7	25	17	19.6
La	-20	-20	23	16	25.4	45	41	40.7
Ce	34	-28	44	42	55.1	100	101	98.8
Pr					6.5			12.0
Nd	-20	-20	-20	21	24.0	48	49	44.5
Sm					5.6			13.0
Eu					0.6			0.1
Gd					5.5			14.8
Tb					1.1			3.2
Dy					6.4			23.1
Ho					1.2			5.0
Er					3.3			16.2
Yb					3.1			18.2
Lu					0.4			2.6
Hf					3.3			6.7
Ta					2.5			2.4
W	-10	-10	-10	13	6.7	12	22	7.5
Pb	33	12	26	32	28.8	44	65	61.9
Bi	-10	-5	-5	-1	1.3	-5	-1	0.3
Th	20	10	13	16	16.7	60	64	61.5
U	15	-10	25	25.7	24.2	35	34.5	32.6

** total iron as Fe_2O_3*

Chemical analyses of the Lisle Granodiorite (R014555) and Meredith Granite (R017895) are not yet available.

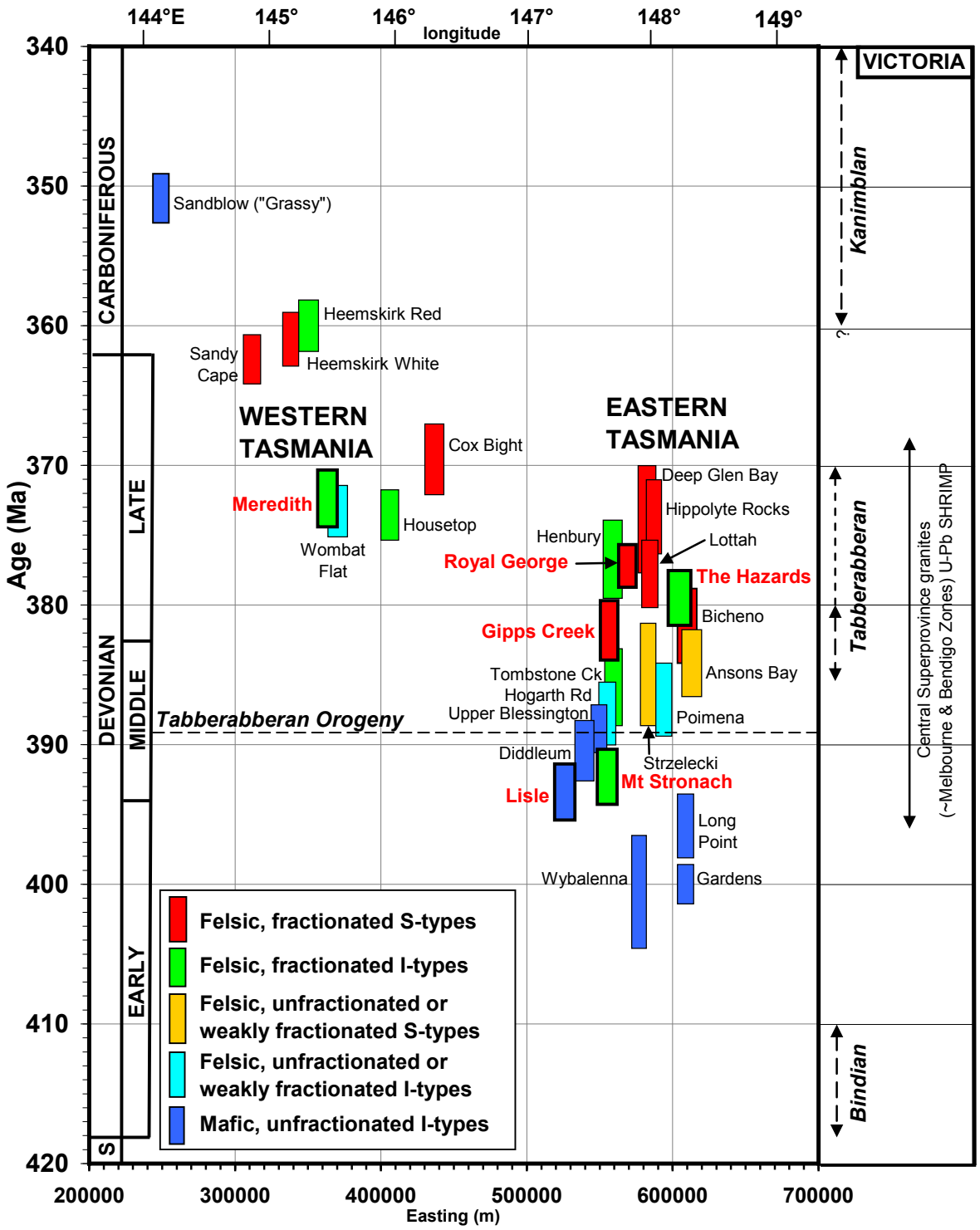

Figure 1.3 *Summary time-space diagram (modified after Black et al., 2005, Figure 7) plotting emplacement age versus easting for Devonian–Carboniferous granites in Tasmania. New data presented in this record shown with heavy outline and red labels; the age uncertainties depicted include the additional component for session-specific calibration uncertainty. Time scale after Tucker at al. (1998), Victorian data after VandenBerg et al. (2000); see Black et al. (2005) for sources.*

2. Eastern Tasmania Terrane

2.1. Lisle Granodiorite

Table 2.1 *Summary of results: Lisle Granodiorite (MRT R014555, GA 2152726).*

GA SampleNo	2152726
MRT Registration No	R014555
MRT Field No	-
Lithology	Biotite-hornblende granodiorite
Stratigraphic Unit	Lisle Granodiorite
Collector	I Woolward
Province/Region	Eastern Tasmanian Terrane
1:250 000 Sheet	LAUNCESTON (SK55-4)
1:100 000 Sheet	ST PATRICKS (8315)
Location (MGA94)	Zone 55, 527712 mE 5432383 mN
Analytical Session	130036 (see Appendix Table A.1 for parameters derived from concurrent measurements of $^{238}U/^{206}Pb$ and $^{207}Pb/^{206}Pb$ reference zircons)
Interpreted Age	393.3 ± 2.0 Ma (95% confidence; 24 analyses of 24 zircons)
Geological Attribution	Magmatic crystallisation
Isotopic Ratio(s) Used	$^{238}U/^{206}Pb$ (^{204}Pb-corrected)

2.1.1. Location details and lithological characteristics

This sample was collected in 2008 from one of several tors cropping out on a small spur, about 3 km south of Lisle Township, northeast Tasmania (Figure 1.1). The sample is a grey even- and medium-grained (~3 mm) granodiorite with scattered angular to irregular finer-grained and darker mafic enclaves up to about 50 mm long. Its magnetic susceptibility (~4.5 x 10^{-3} SI) suggests that it contains some magnetite.

In thin section, it consists mainly of anhedral quartz, generally subhedral plagioclase and subordinate microcline, biotite (α pale yellow-brown, β and γ dark brown) and hornblende (α pale yellow, β and γ pale green). Plagioclase is usually strongly zoned with more calcic and locally turbid or partly sericitised cores (to ~An_{45}), and commonly also displays oscillatory zoning. Opaque grains (~50–150 μm) are generally equant; some are cubic euhedra (magnetite and possibly pyrite). Accessory zircon, monazite (?), apatite and traces of carbonate were noted. Some biotite is partly altered to pale green chlorite with rods of titanite aligned in the cleavage. An enclave is finer-grained (~250 μm) and mineralogically similar, but contains more abundant hornblende and less biotite and quartz.

A chemical analysis of the dated sample is not yet available. However, the sample appears typical of the Lisle Granodiorite, of which fourteen published analyses of unaltered samples (Roach, 1994; Bottrill, 1996) are generally metaluminous, unfractionated I-type granodiorites (e.g. SiO_2 64.2–67.1%, FeO_{tot} 3.99–4.74%, Rb 72–87 ppm, Sr 220–376 ppm).

2.1.2. Zircon description

Zircons from this sample are predominantly euhedral to subhedral and range from equant to prismatic with very few elongate crystals (Figure 2.1). Aspect ratios are commonly 1:2 but range up to ~1:5, and long axes are 50–200 µm. In transmitted light, the crystals are predominantly transparent and colourless or light yellow-brown.

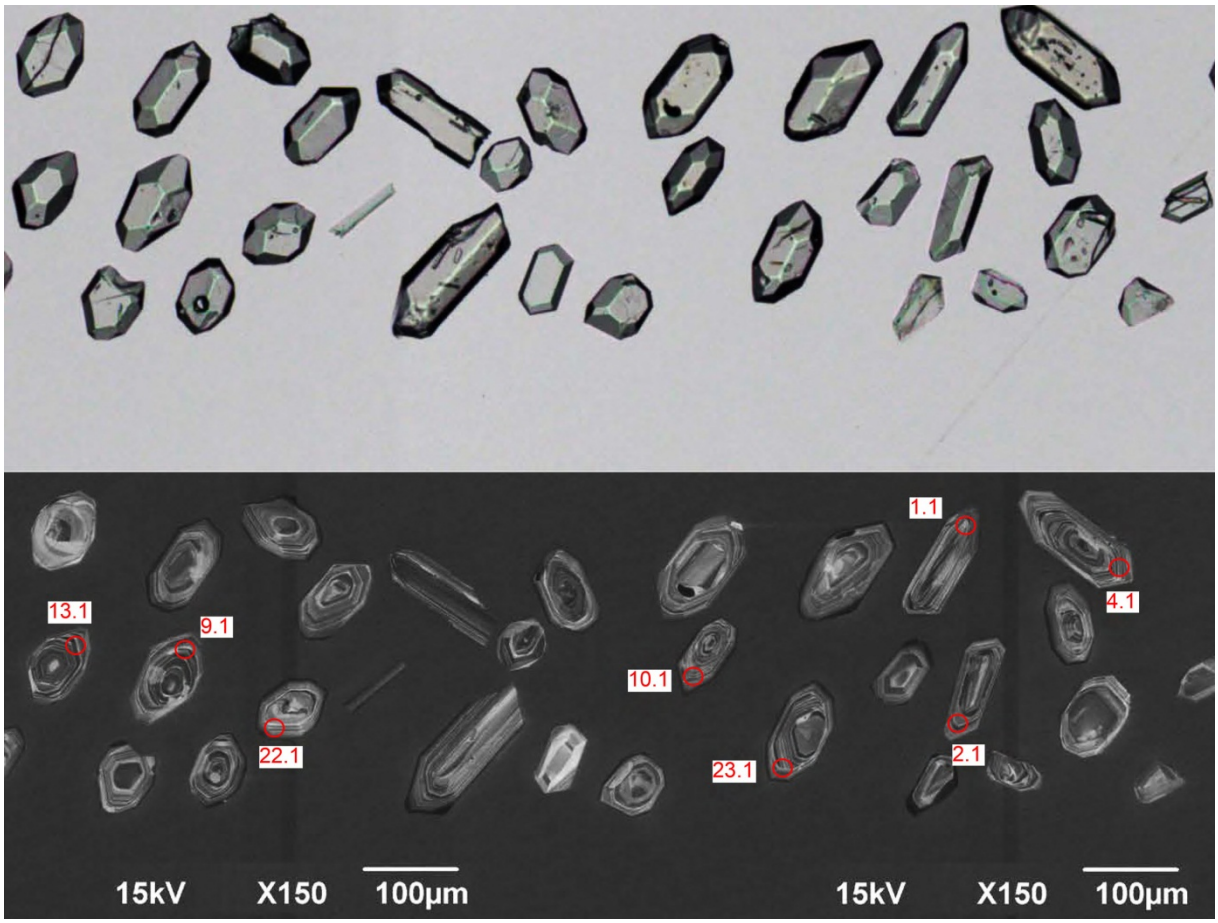

Figure 2.1 *Representative zircons from the Lisle Granodiorite (MRT R014555, GA 2152726). Transmitted light image is shown in the upper half; cathodoluminescence image in the lower half. SHRIMP analysis sites are labelled.*

Cathodoluminescence images reveal a moderately uniform intensity of emission, and are dominated by medium contrast oscillatory zoning parallel to the crystals faces, typical of magmatic zircon. A few crystals feature cores of either low or bright emission, which have sharp, disconformable contacts with their concentrically zoned overgrowths, likely representing inheritance.

2.1.3. U–Pb isotopic results

A total of 28 analyses were collected from 28 zircon crystals, the results of which are presented in Table 2.2 and Figure 2.2. The analysed zircons are characterised by moderate U contents (168–580 ppm, median = 309 ppm), and moderate Th/U (0.31–1.55, median = 0.46).

Twenty-seven analyses have uniformly low $^{206}Pb_c$ (maximum 0.28%, median = 0.08%) and can be divided into three groups:

- Group 1 comprises 24 analyses of 24 zircons with individual $^{238}U/^{206}Pb$ ages between c. 401 Ma and c. 386 Ma, which yield a weighted mean age of 393.3 ± 2.0 Ma (MSWD = 1.08);
- Group 2 comprises three analyses from three grains, with individual $^{238}U/^{206}Pb$ ages of 561 ± 5 Ma (1σ), 561 ± 6 Ma (1σ), and 572 ± 5 Ma (1σ), and
- Group 3 is a single analysis (20.1.1) with an age of 381.2 ± 3.8 Ma (1σ).

2.1.4. Geochronological interpretation

The weighted mean $^{238}U/^{206}Pb$ age of 393.3 ± 2.0 Ma, for the 24 analyses in Group 1, is interpreted as the magmatic crystallisation age of the Lisle Granodiorite. The three analyses in Group 2 are interpreted as inherited individuals of Neoproterozoic age. The single analysis in Group 3 is interpreted to have been affected by post-crystallisation loss of radiogenic Pb.

The uncertainty in the weighted mean $^{238}U/^{206}Pb$ age for Group 1 quoted above includes a component arising from the session-specific calibration uncertainty as determined on the $^{238}U/^{206}Pb$ reference zircon (in this case, 0.30% (2σ) on TEMORA2 in session 130036). However, this calibration uncertainty should be neglected when comparing weighted mean $^{238}U/^{206}Pb$ ages determined during the same analytical session, because that component of the 95% confidence interval is common to each weighted mean from that session. Consequently, the discussion below shows (in square brackets) narrowed 95% confidence intervals specific to weighted mean $^{238}U/^{206}Pb$ ages determined from session 130036, for the sole purpose of intra-session comparisons.

In comparison with other new SHRIMP zircon $^{238}U/^{206}Pb$ magmatic crystallisation ages presented in this Record, the 393.3 ± [1.6]2.0 Ma Lisle Granodiorite is indistinguishable from the 392.2 ± [1.5]1.9 Ma Mount Stronach Granite. It is distinguishably older than the 381.7 ± [1.8]2.2 Ma Gipps Creek Granite, the 379.3 ± [1.6]1.9 Ma Hazards Granite, the 377.1 ± [1.5]1.8 Ma Royal George Granite and the 372.2 ± [1.6]1.9 Ma Meredith Granite.

The magmatic crystallisation age of 393.3 ± 2.0 Ma for this occurrence of the Lisle Granodiorite is within error of an existing SHRIMP zircon $^{238}U/^{206}Pb$ age of 390.4 ± 2.2 Ma for the nearby (and chemically similar) Diddleum Granodiorite (Black et al., 2005). However, the Lisle Granodiorite is distinguishably older than two other Scottsdale Batholith plutons: the 387.8 ± 2.3 Ma Hogarth Road Granite and the 385.9 ± 2.8 Ma Tombstone Creek Granite (Black et al., 2005, see Figure 1.3).

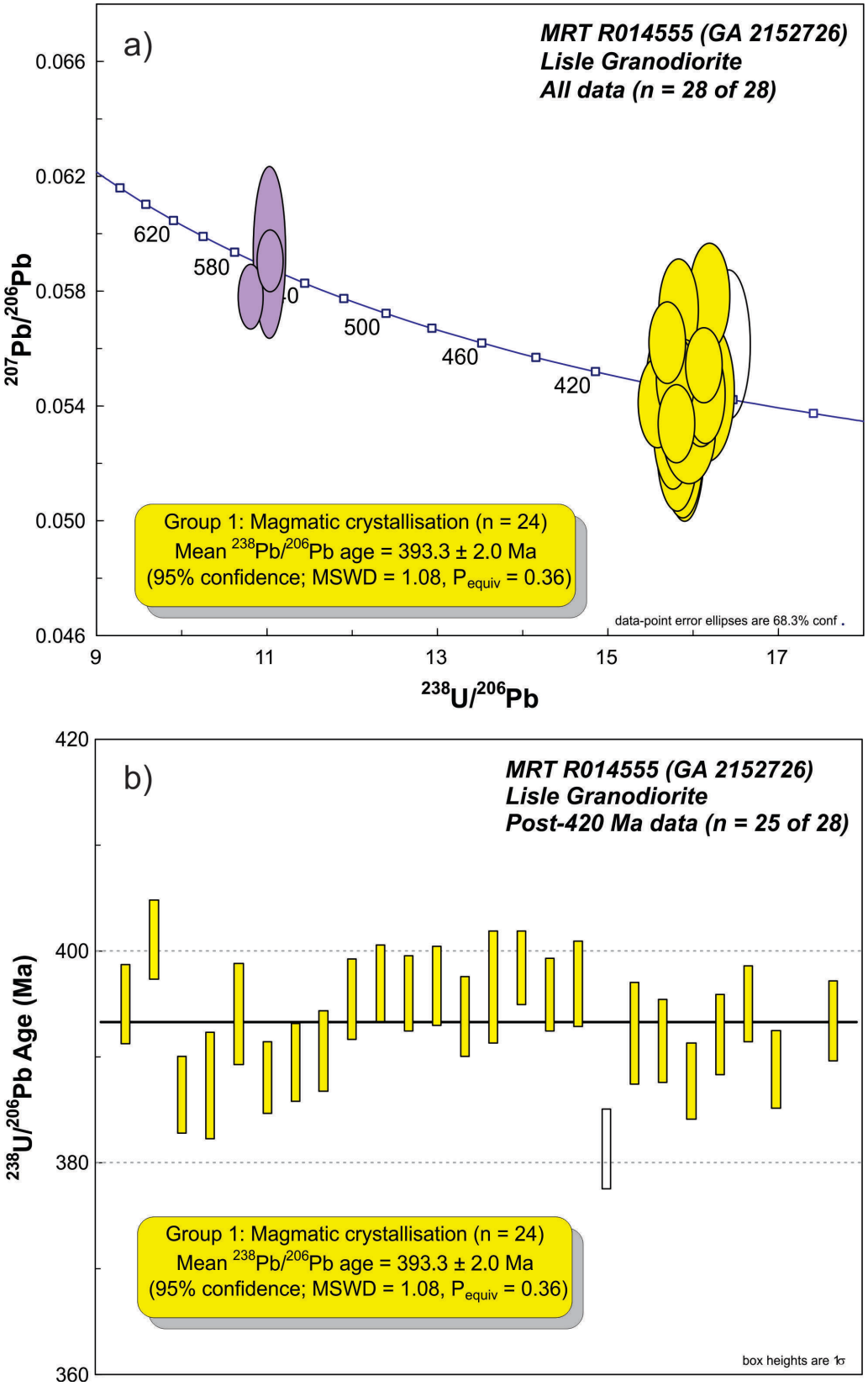

Figure 2.2 *SHRIMP U–Pb data for zircons from the Lisle Granodiorite (MRT R014555, GA 2152726). (a) Tera-Wasserburg concordia diagram; (b) Post-420 Ma $^{238}U/^{206}Pb$ ages in order of acquisition. Yellow fill denotes Group 1 (magmatic crystallisation); purple fill denotes Group 2 (inheritance); white fill denotes Group 3 (analysis affected by loss of radiogenic Pb). Heavy black line: weighted mean $^{238}U/^{206}Pb$ age.*

2.1.5. Discussion

The Lisle Granodiorite is a small poorly outcropping body exposed in the floor of the Lisle valley, surrounded by a contact aureole of very resistant Mathinna Supergroup biotite-cordierite hornfels which forms an amphitheatre-like topographic feature. The hornfels is derived from the Lone Star Siltstone (part of the Panama Group and Mathinna Supergroup), which elsewhere contains Silurian (Ludlow) graptolites (Seymour et al., 2011). Modally the body ranges from granodiorite to tonalite, but it contains numerous enclaves of quartz diorite composition, and dykes of more felsic granite and aplite (Bottrill, 1996).

The Lisle Granodiorite is unfoliated, and Bottrill (1996) considered that it post-dates folding and regional metamorphism in the Mathinna Supergroup.

Small stocks of similar granodiorite crop out about 7 km to the NNE at Lone Star Creek, near Panama Ridge and at Golconda. The large Diddleum Granodiorite, which crops out ~8 km to the east, is chemically similar to the Lisle Granodiorite, but tends to have lower Na_2O and Sr and higher K_2O and Rb and Al_2O_3 and contains a distinct grain foliation.

The Lisle valley produced at least 2.7 t, and possibly more than 8 t of gold, mostly between 1878 and 1902, almost all from placers including possible Tertiary lake deposits (Twelvetrees, 1909; Bottrill, 1996). Auriferous quartz is relatively rare at Lisle, suggesting that gold has not originated from quartz veins in the Mathinna Supergroup, as is common in northeastern Tasmania. Thureau (1882) and Twelvetrees (1909) favoured an origin in the contact aureole near the contact with the granodiorite. Montgomery (1894) found some gold in quartz veins within granitic rocks, and Bottrill (1996) found anomalous gold and minor pyrite in a brecciated zone within granodiorite. Reid (1926) postulated that most of the alluvial gold was secondary, having been precipitated from chlorine-bearing groundwater. Roach (1994) concluded that the gold was derived from quartz-sulphide veins within both the granodiorite and the surrounding Mathinna Supergroup, and had been strongly concentrated in the alluvials due to the unusual local topography and hydrology and possibly by biologically induced precipitation of dissolved gold in groundwater.

Seymour et al. (2011) attributed the SW-vergent folds and associated SW-directed thrusts in the southern part of the Lone Star Siltstone to their TaD_1 (Tabberabberan D_1) deformation, and suggested that the lack of overprinting structural relationships (common elsewhere in the Panama Group) was due to reactivation of earlier TaD_{1-2} structures. In the vicinity of the Lisle Granodiorite, the inferred TaD_3 fold axes and cleavages are bowed around the pluton. It was suggested that this was due to forceful (rather than passive) emplacement of the granodiorite 'at a structural level when folds started forming and when cleavage was completely developed', i.e. intrusion was 'late-TaD_3 in relative age rather than completely post-tectonic.'

The 393.3 ± 2.0 Ma age the Lisle Granodiorite is consistent with a close relationship with the Scottsdale Batholith (Figures 1.1 and 1.3) and in particular its oldest dated pluton, the Diddleum Granodiorite (390.4 ± 2.2 Ma; Black et al., 2005), despite some geochemical differences. It also places a maximum age on the local primary gold mineralisation.

Black et al. (2005) noted that eastern Tasmanian granites older than ~389 Ma, including the Diddleum Granodiorite, generally contain a grain foliation defined by alignment of mafic minerals, which they correlated with the earliest Tabberabberan deformation (D_3 of Reed, 2001 and TaD_1 of Seymour et al., 2011). The apparent absence of any such foliation in the ~393 Ma Lisle Granodiorite is therefore

anomalous. Late syntectonic (TaD_3) emplacement, suggested by Seymour et al. (2011), is difficult to reconcile with the SHRIMP age.

Table 2.2 *SHRIMP U–Pb zircon data from Lisle Granodiorite (MRT R014555, GA 2152726).*

Grain.area .replicate	$^{206}Pb_c$ (%)	U (ppm)	Th (ppm)	$^{232}Th/^{238}U$	$^{238}U/^{206}Pb$	± 1σ (%)	$^{207}Pb/^{206}Pb$	± 1σ (%)	$^{238}U/^{206}Pb$ Age (Ma)	± 1σ (Ma)	disc (%)
Group 2: inherited individuals (n = 3)											
27.1.1	-0.10	168	183	1.12	10.994	1.15	0.05929	3.35	561.2	6.2	+3
29.1.1	0.11	415	623	1.55	10.773	0.92	0.05775	1.29	572.2	5.0	-10
30.1.1	0.05	458	142	0.32	11.005	0.91	0.05901	1.21	560.7	4.9	+1
Group 1: magmatic crystallisation (n = 24)											
1.1.1	-0.25	359	160	0.46	15.827	0.97	0.05728	2.08	395.0	3.7	+22
2.1.1	-0.02	387	165	0.44	15.578	0.97	0.05402	1.93	401.1	3.8	-8
3.1.1	-0.28	378	167	0.46	16.188	0.96	0.05777	2.11	386.4	3.6	+27
4.1.1	-0.02	284	130	0.47	16.151	1.34	0.05443	3.00	387.3	5.0	+0
5.1.1	0.05	499	336	0.69	15.865	1.25	0.05455	2.06	394.0	4.8	-0
6.1.1	-0.08	580	304	0.54	16.119	0.90	0.05534	1.56	388.0	3.4	+9
7.1.1	-0.04	296	135	0.47	16.058	0.98	0.05464	2.36	389.4	3.7	+2
8.1.1	0.13	264	91	0.36	16.012	1.01	0.05389	2.64	390.5	3.8	-7
9.1.1	0.20	282	164	0.60	15.808	0.99	0.05239	2.73	395.4	3.8	-32
10.1.1	0.03	355	182	0.53	15.745	0.95	0.05412	2.26	396.9	3.6	-6
11.1.1	0.06	413	122	0.31	15.785	0.92	0.05484	1.86	396.0	3.5	+2
12.1.1	0.21	301	134	0.46	15.755	0.97	0.05308	2.60	396.7	3.7	-20
13.1.1	0.28	289	117	0.42	15.875	0.99	0.05227	2.89	393.8	3.8	-33
14.1.1	-0.05	310	165	0.55	15.761	1.38	0.05467	2.85	396.6	5.3	+1
17.1.1	-0.16	444	224	0.52	15.685	0.90	0.05613	1.69	398.4	3.5	+13
18.1.1	0.05	476	288	0.63	15.791	0.90	0.05329	1.71	395.8	3.5	-17
19.1.1	0.19	218	82	0.39	15.748	1.05	0.05460	3.26	396.9	4.0	-0
21.1.1	0.15	307	134	0.45	15.942	1.28	0.05305	2.30	392.2	4.9	-19
22.1.1	-0.06	239	94	0.41	15.972	1.03	0.05443	3.10	391.5	3.9	-1
23.1.1	-0.02	329	141	0.44	16.134	0.96	0.05431	2.10	387.7	3.6	-1
24.1.1	0.15	267	119	0.46	15.947	1.00	0.05370	2.55	392.1	3.8	-10
25.1.1	0.09	341	144	0.44	15.825	0.93	0.05400	2.27	395.0	3.6	-7
26.1.1	0.09	297	118	0.41	16.086	0.98	0.05423	2.13	388.8	3.7	-2
28.1.1	0.12	297	138	0.48	15.893	0.99	0.05255	3.38	393.4	3.8	-28
Group 3: affected by loss of radiogenic Pb (n = 1)											
20.1.1	-0.30	258	124	0.50	16.414	1.02	0.05606	3.08	381.2	3.8	+17

2.2. Mount Stronach Granite

Table 2.3 *Summary of results: Mount Stronach Granite (MRT R013228, GA 2152729).*

GA SampleNo	2152729
MRT Registration No	R013228
MRT Field No	NJ111
Lithology	Alkali feldspar granite
Stratigraphic Unit	Mount Stronach Granite
Collector	JL Everard
Province/Region	Eastern Tasmanian Terrane
1:250 000 Sheet	LAUNCESTON (SK55-4)
1:100 000 Sheet	FORESTER (8415)
Location (MGA94)	Zone 55, 548472 mE, 5446433 mN
Analytical Session	130036 (see Appendix Table A.1 for parameters derived from concurrent measurements of $^{238}U/^{206}Pb$ and $^{207}Pb/^{206}Pb$ reference zircons)
Interpreted Age	392.2 ± 1.9 Ma (95% confidence; 23 analyses of 22 zircons)
Geological Attribution	Magmatic crystallisation
Isotopic Ratio(s) Used	$^{238}U/^{206}Pb$ (^{204}Pb-corrected)

2.2.1. Location details and lithological characteristics

The sample was collected in 2007 from a fresh road cutting in a new forestry spur road off Old Waterhouse Road, about 6 km east-northeast of Scottsdale, northeastern Tasmania (Figure 1.1). It is a fresh white to very pale pink, fine-grained (~2–3 mm) equigranular, fractionated granite, consisting of quartz, plagioclase (albite to oligoclase), alkali feldspar (including microcline with microperthitic albite inclusions), and pale yellow-brown to very dark brown, almost opaque biotite (≤1.5 mm). Plagioclase cores and alkali feldspar grains are commonly turbid due to sericitisation, and biotite is partly altered to chlorite. Traces of secondary muscovite are present.

A chemical analysis (Table 1.2) shows that it is a very felsic, fractionated, very weakly peraluminous alkali feldspar granite.

2.2.2. Zircon description

Zircons from this sample range from euhedral to anhedral, with external morphologies ranging from rounded and anhedral grains, through to euhedral prisms with pyramidal terminations (Figure 2.3). Many crystals are broken or fractured — these are often dark brown to black and opaque in transmitted light. Zircons are generally clear and colourless to light yellow and orange and range from ~50 µm to ~250 µm in length with aspect ratios ranging between 1:1 and 1:3.

In cathodoluminescence images, the grains are characterised by low to moderate emission, are dominantly oscillatory zoned in nature, with lesser grains exhibiting broad banding parallel to their long

axes or sector zoning. Inherited cores are evident in a few grains, and are most obvious where their emission contrasts with the surrounding magmatic overgrowths.

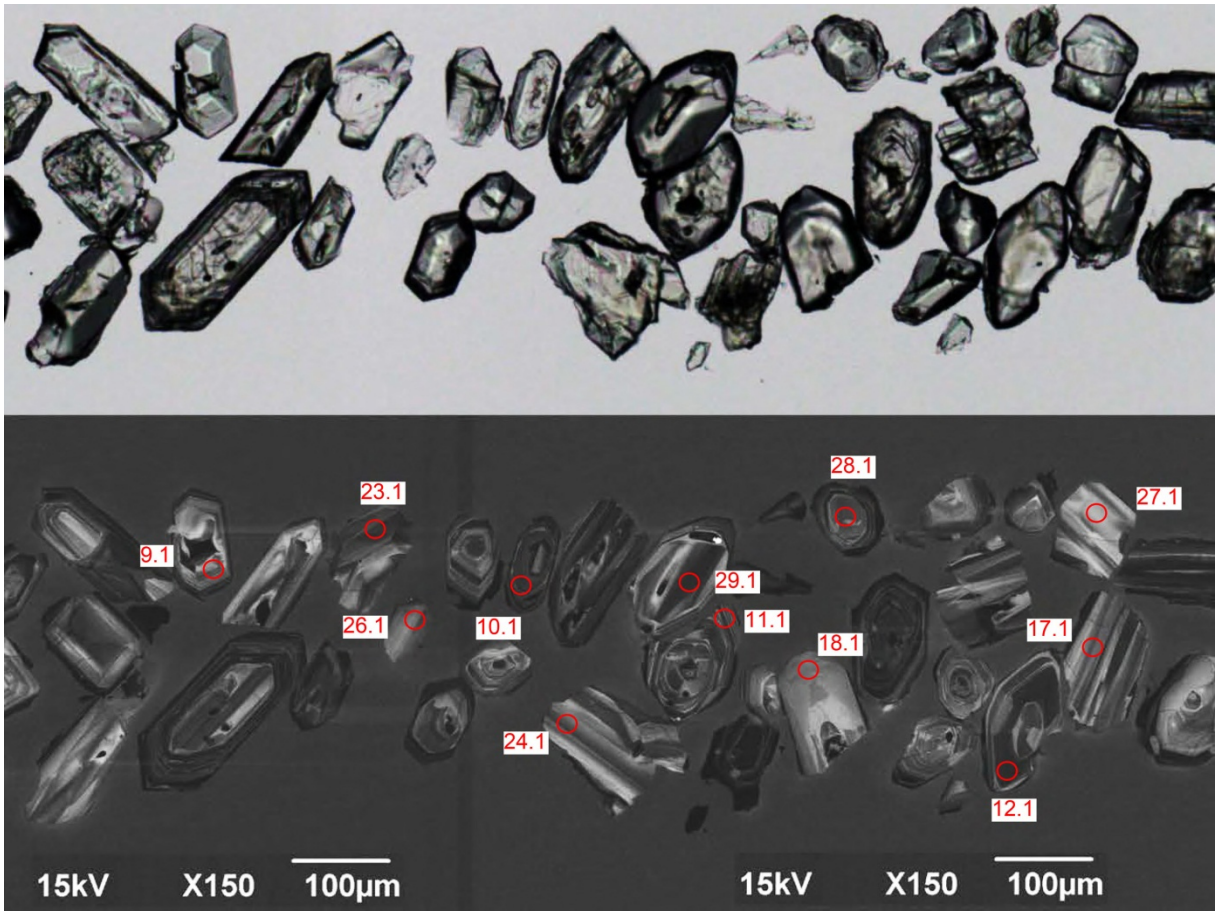

Figure 2.3 *Representative zircons from the Mount Stronach Granite (MRT R013228, GA 2152729). Transmitted light image is shown in the upper half; cathodoluminescence image in the lower half. SHRIMP analysis sites are labelled.*

2.2.3. U–Pb isotopic results

A total of 29 analyses were collected from 28 zircon crystals, the results of which are presented in Table 2.4 and Figure 2.4. One grain (14) was analysed twice. The analysed zircons are characterised by low to high U contents (109–1308 ppm, median = 320 ppm), and low to moderate Th/U (0.05–0.89, median = 0.42). Five analyses were characterised by high $^{206}Pb_c$ (>0.9%). The data obtained from these five analyses are interpreted as unreliable and are not considered further.

The remaining 24 analyses have uniformly low $^{206}Pb_c$ (maximum 0.34%) and can be divided into two groups:

- Group 1 comprises 23 analyses of 22 zircons with individual $^{238}U/^{206}Pb$ ages between c. 399 Ma and c. 385 Ma, which yield a weighted mean age of 392.2 ± 1.9 Ma (MSWD = 1.13), and
- Group 2 comprises a single analysis with a $^{238}U/^{206}Pb$ age of 484 ± 4 Ma (1σ).

2.2.4. Geochronological interpretation

The $^{238}U/^{206}Pb$ weighted mean age of 392.2 ± 1.9 Ma, for the 23 analyses in Group 1, is interpreted as the best estimate of the age of magmatic crystallisation of the Mount Stronach Granite. The single 484 ± 4 Ma (1σ) analysis in Group 2 is interpreted as an inherited individual of Ordovician age.

The uncertainty in the weighted mean $^{238}U/^{206}Pb$ age for Group 1 quoted above includes a component arising from the session-specific calibration uncertainty as determined on the $^{238}U/^{206}Pb$ reference zircon (in this case, 0.30% (2σ) on TEMORA2 in session 130036). However, this calibration uncertainty should be neglected when comparing weighted mean $^{238}U/^{206}Pb$ ages determined during the same analytical session, because that component of the 95% confidence interval is common to each weighted mean from that session. Consequently, the discussion below shows (in square brackets) narrowed 95% confidence intervals specific to weighted mean $^{238}U/^{206}Pb$ ages determined from session 130036, for the sole purpose of intra-session comparisons.

In comparison with other new SHRIMP zircon $^{238}U/^{206}Pb$ magmatic crystallisation ages presented in this Record, the 392.2 ± [1.5]1.9 Ma Mount Stronach Granite is indistinguishable from the 393.3 ± [1.6]2.0 Ma Lisle Granodiorite. It is distinguishably older than the 381.7 ± [1.8]2.2 Ma Gipps Creek Granite, the 379.3 ± [1.6]1.9 Ma Hazards Granite, the 377.1 ± [1.5]1.8 Ma Royal George Granite and the 372.2 ± [1.6]1.9 Ma Meredith Granite.

The magmatic crystallisation age of 392.2 ± 1.9 Ma for this occurrence of the Mount Stronach Granite can be compared to the existing SHRIMP zircon $^{238}U/^{206}Pb$ ages of members of the Scottsdale Batholith reported by Black et al. (2005). The 392.2 ± 1.9 Ma Mount Stronach Granite is distinguishably older than the 385.9 ± 2.8 Ma Tombstone Creek Granite, the 387.8 ± 2.3 Ma Hogarth Road Granite and the 388.9 ± 1.6 Ma Upper Blessington Granodiorite, but is indistinguishable from the 390.4 ± 2.2 Ma Diddleum Granodiorite (Figure 1.3).

2.2.5. Discussion

The Mount Stronach Granite crops out over ~25km^2 and is the most felsic pluton of the Scottsdale Batholith. Minor molybdenum mineralisation is associated with the granite at Mount Stronach. The granite has previously been described by Robinson (1982) and McClenaghan (1989, p. 259). Robinson (1982) and McClenaghan (1994a, b) have mapped the local pluton geometry as a partly concentric ‘zonal arrangement’, comprising a central core of medium-grained porphyritic biotite granite (Hogarth Road Granite) partly surrounded by coarse-grained pinkish biotite granite (Russells Road Granite) and in turn the semi-circular or crudely horseshoe-shaped tract of the Mount Stronach Granite (Figure 1.1). Contacts of the Mount Stronach Granite with the Russells Road Granite and, to the east, with the Tulendeena Granodiorite are poorly exposed and relative age relationships have not been established from field relations.

Previous SHRIMP dating of the Scottsdale Batholith appeared to show that it was emplaced over 4–5 Myr, and that successive plutons became progressively more felsic (Black et al., 2005; see Figure 1.3). Furthermore, Sr and Nd isotope ratios were interpreted as indicating a small but progressively increasing sedimentary component to the granites (Black et al., 2010). On this basis, it was thought that the very felsic Mount Stronach Granite might be the youngest pluton of the Batholith (although its relatively high εNd value of -0.7 lies off the trend defined by the other plutons).

The magmatic crystallisation age of 392.2 ± 1.9 Ma for the Mount Stronach Granite is thus unexpectedly old, and is also surprising in view of the absence of a tectonic grain foliation, which is present in the younger Upper Blessington Granodiorite and other pre ~389 Ma granites in eastern Tasmania (Black et al., 2005). An age older than the Hogarth Road Granite is, however, consistent with the zonal pluton geometry described above. The old age and low εNd suggests that the Mount Stronach Granite has a different petrogenesis from the other plutons. In particular, a genetic relationship with the ~6 Myr younger Tombstone Creek Granite (as implied by McClenaghan, 1989, p. 259) is unlikely.

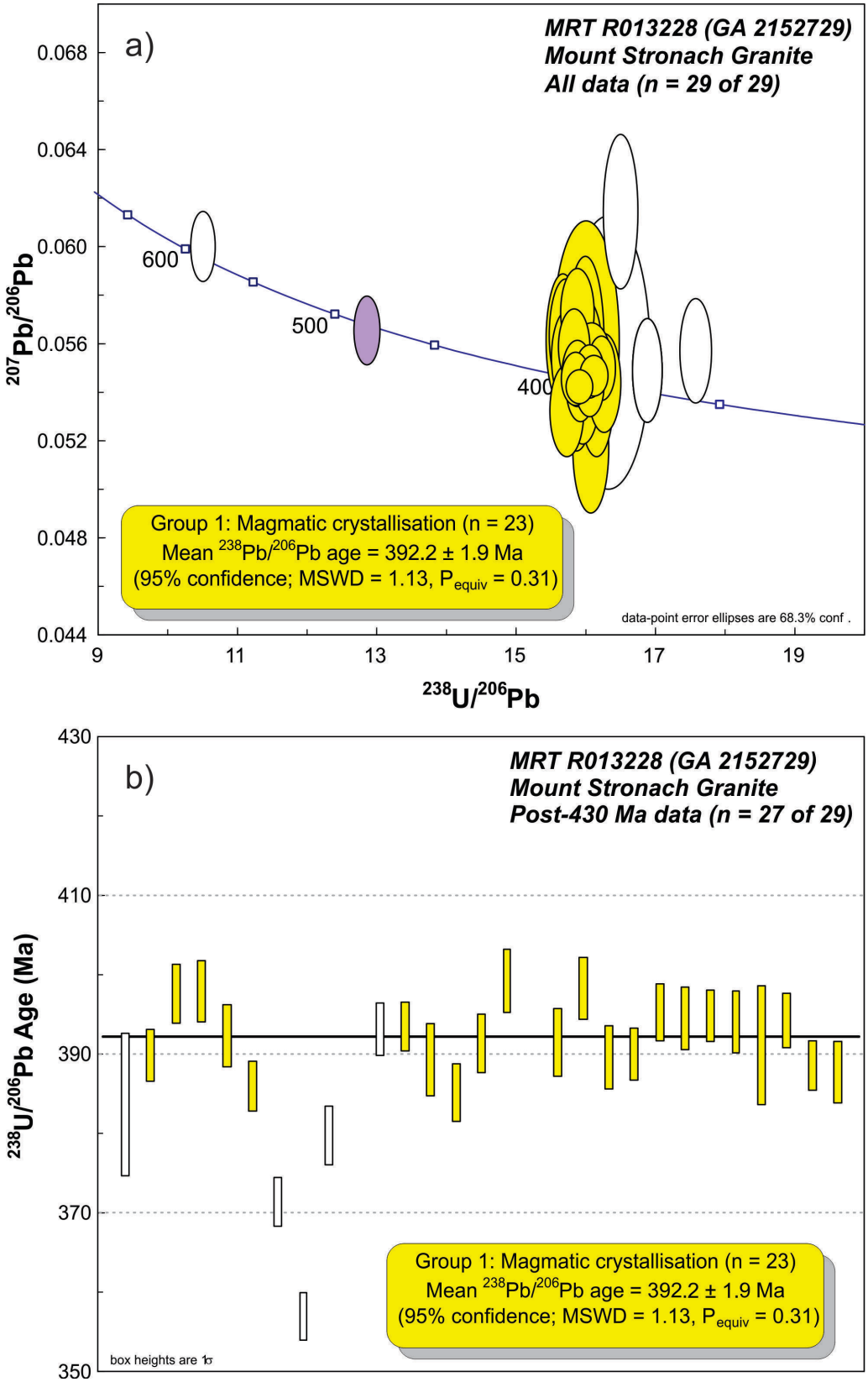

Figure 2.4 *SHRIMP U–Pb data for zircons from the Mount Stronach Granite (MRT R013228, GA 2152729). (a) Tera-Wasserburg concordia diagram; (b) Post-430 Ma $^{238}U/^{206}Pb$ ages in order of acquisition. Yellow fill denotes Group 1 (magmatic crystallisation); purple fill denotes Group 2 (inheritance); white fill denotes relatively high common Pb ($^{206}Pb_c$ >0.9%). Heavy black line: weighted mean $^{238}U/^{206}Pb$ age.*

Table 2.4 *SHRIMP U–Pb zircon data from Mount Stronach Granite (MRT R013228, GA 2152729).*

Grain.area .replicate	$^{206}Pb_c$ (%)	U (ppm)	Th (ppm)	$^{232}Th/^{238}U$	$^{238}U/^{206}Pb$	± 1σ (%)	$^{207}Pb/^{206}Pb$	± 1σ (%)	$^{238}U/^{206}Pb$ Age (Ma)	± 1σ (Ma)	disc (%)
Group 2: inherited individual (n = 1)											
19.1.1	0.11	379	192	0.52	12.826	0.93	0.05647	1.68	484.0	4.3	-3
Group 1: magmatic crystallisation (n = 23)											
2.1.1	0.12	807	346	0.44	16.043	0.87	0.05477	1.33	389.8	3.3	+3
3.1.1	0.33	412	145	0.36	15.720	0.96	0.05534	2.34	397.6	3.7	+7
4.1.1	0.07	320	82	0.27	15.708	1.00	0.05312	2.38	397.9	3.9	-20
5.1.1	0.01	292	135	0.48	15.939	1.03	0.05400	2.76	392.3	3.9	-6
6.1.1	0.25	1142	316	0.29	16.209	0.84	0.05489	1.61	385.9	3.1	+6
11.1.1	0.16	642	253	0.41	15.905	0.86	0.05412	1.77	393.1	3.3	-5
12.1.1	0.13	1308	705	0.56	15.892	0.81	0.05412	0.85	393.4	3.1	-5
13.1.1	0.11	361	207	0.59	16.068	1.20	0.05507	2.04	389.2	4.5	+6
14.1.1	-0.02	299	159	0.55	16.246	0.97	0.05428	2.50	385.1	3.6	-1
17.1.1	0.03	292	67	0.24	15.980	0.97	0.05567	2.49	391.3	3.7	+11
18.1.1	-0.16	236	70	0.31	15.654	1.03	0.05606	3.24	399.2	4.0	+13
20.1.1	-0.17	176	32	0.19	15.976	1.12	0.05606	4.09	391.4	4.3	+14
21.1.1	-0.17	253	63	0.26	15.694	1.01	0.05624	2.76	398.2	3.9	+14
22.1.1	0.01	213	39	0.19	16.054	1.05	0.05156	3.44	389.5	4.0	-48
23.1.1	0.34	658	231	0.36	16.037	0.86	0.05415	1.55	389.9	3.3	-3
24.1.1	-0.12	377	158	0.43	15.816	0.93	0.05578	1.85	395.2	3.6	+11
14.2.1	0.01	229	116	0.53	15.848	1.03	0.05383	2.90	394.5	3.9	-9
25.1.1	0.36	814	129	0.16	15.834	0.84	0.05445	1.34	394.8	3.2	-1
26.1.1	-0.10	257	107	0.43	15.866	1.02	0.05723	2.08	394.0	3.9	+22
27.1.1	0.02	109	20	0.19	15.991	1.98	0.05601	5.92	391.0	7.5	+14
28.1.1	-0.01	474	136	0.30	15.860	0.91	0.05468	1.67	394.2	3.5	+1
29.1.1	0.04	1063	916	0.89	16.099	0.83	0.05459	1.01	388.5	3.1	+2
30.1.1	0.15	250	143	0.59	16.136	1.03	0.05389	3.28	387.6	3.9	-6
Not considered: high Pb_c (n = 5)											
1.1.1	2.17	245	107	0.45	16.312	2.41	0.05554	6.74	383.6	9.0	+12
7.1.1	2.83	978	575	0.61	16.868	0.85	0.05481	2.59	371.3	3.1	+8
9.1.1	1.36	296	121	0.42	16.485	1.00	0.06140	3.45	379.6	3.7	+43
10.1.1	1.30	943	43	0.05	10.456	1.12	0.05995	1.60	588.8	6.3	+2
8.1.1	0.96	631	304	0.50	17.573	0.87	0.05562	2.59	356.8	3.0	+19

2.3. Royal George Granite

Table 2.5 *Summary of results: Royal George Granite (MRT R004491, GA 2152728).*

GA SampleNo	2152728
MRT Registration No	R004491
MRT Field No	SG35
Lithology	Alkali feldspar granite
Stratigraphic Unit	Royal George Granite
Collector	JL Everard
Province/Region	Eastern Tasmanian Terrane
1:250 000 Sheet	OATLANDS (SK55-6)
1:100 000 Sheet	ST PAULS (8414)
Location (MGA94)	Zone 55, 572852 mE, 5367173 mN
Analytical Session	130036 (see Appendix Table A.1 for parameters derived from concurrent measurements of $^{238}U/^{206}Pb$ and $^{207}Pb/^{206}Pb$ reference zircons)
Interpreted Age	377.1 ± 1.8 Ma (95% confidence; 24 analyses of 23 zircons)
Geological Attribution	Magmatic crystallisation
Isotopic Ratio(s) Used	$^{238}U/^{206}Pb$ (^{204}Pb-corrected)

2.3.1. Location details and lithological characteristics

The sample was collected in 2001 using explosives, from outcropping tors on the north flank of Deer Hill, about 3 km south-southwest of Royal George, central eastern Tasmania (Figure 1.1). The sample is a fine- to medium-grained sparsely porphyritic granite with scattered tabular K-feldspar phenocrysts (≤20 mm), equant smoky quartz phenocrysts (≤ 8 mm) and incipient green pinite alteration of cream feldspars. The groundmass consists of K-feldspar (microperthite), plagioclase (albite) and quartz with common anhedral tourmaline (ε colourless to faintly blue, ω pale brown) and sparse ragged booklets of biotite (α nearly colourless, β and γ reddish-brown) with zircon inclusions. K-feldspar and most plagioclase is turbid and partly sericitised.

Chemically (Table 1.2) it is a strongly fractionated peraluminous granite with ASI and trace element geochemistry indicating an S-type character.

2.3.2. Zircon description

Zircon crystals recovered from this sample range from euhedral to anhedral, with external morphologies ranging from rounded grains, through euhedral prisms and elongate needle-like crystals (Figure 2.5). Zircons are generally clear and colourless to various shades of yellow-brown in transmitted light. There is a wide range of aspect ratios (width:length), from 1:1 up to 1:8, with long axes 100–400 µm.

In cathodoluminescence images, a large proportion of grains display oscillatory zoning patterns, with more elongate crystals characterised by broader planar banding parallel to the long axes. A few grains display mottled interiors, or wavy banding patterns. In some grains, the central region is strongly luminescent and structureless while the outer regions have a weaker luminescence and are concentrically zoned. This gives the impression that these grains comprise an inherited core and rim.

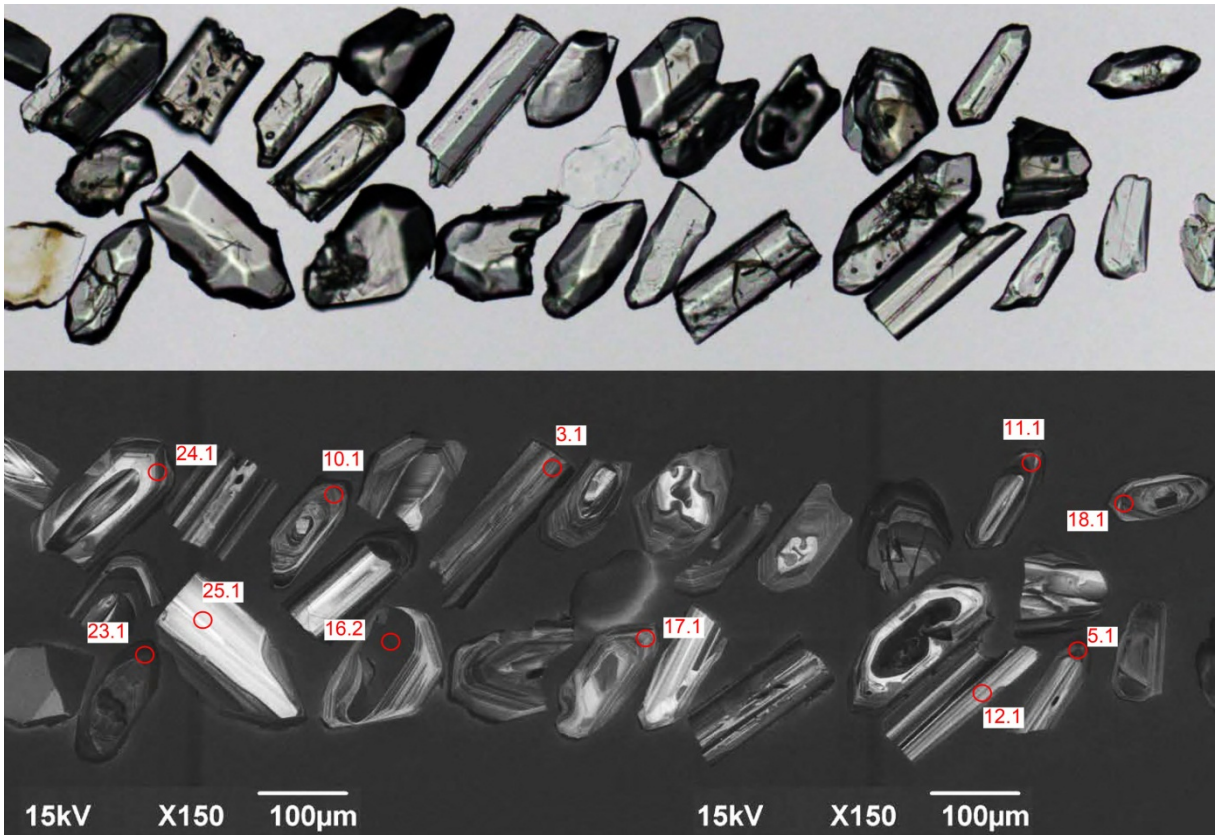

Figure 2.5 *Representative zircons from the Royal George Granite (MRT R004491, GA 2152728). Transmitted light image is shown in the upper half; cathodoluminescence image in the lower half. SHRIMP analysis sites are labelled.*

2.3.3. U–Pb isotopic results

A total of 28 analyses were collected from 25 zircon crystals, the results of which are presented in Table 2.6 and Figure 2.6. Three grains (13, 14, and 20) were analysed twice. The analysed zircons are characterised by low to moderate U contents (61–987 ppm, median = 354 ppm), and moderate Th/U (0.12–1.17, median = 0.27). An identifiably young outlier (4.1.1) was affected by instrument instability. Its $^{238}U/^{206}Pb$ date is unreliable, and is not considered further.

The remaining 27 analyses have uniformly low $^{206}Pb_c$ (maximum 0.66%) and can be divided into three groups:

- Group 1 consists of 24 analyses of 23 zircons with individual $^{238}U/^{206}Pb$ ages between c. 385 Ma and c. 369 Ma, which yield a weighted mean age of 377.1 ± 1.8 Ma (MSWD = 1.10);
- Group 2 comprises two analyses with individual $^{238}U/^{206}Pb$ ages of 522 ± 5 Ma (1σ) and 791 ± 25 Ma (1σ), and

- Group 3 is a single analysis with a $^{207}Pb/^{206}Pb$ age of 2851 ± 12 Ma (1σ).

2.3.4. Geochronological interpretation

The weighted mean $^{238}U/^{206}Pb$ age of 377.1 ± 1.8 Ma, for the 24 analyses in Group 1, is interpreted as the best estimate of the age of magmatic crystallisation of the Royal George Granite. The two analyses, 522 ± 5 Ma (1σ) and 791 ± 25 Ma (1σ) in Group 2, are interpreted as inherited individuals of Cambrian and Neoproterozoic age, respectively. The single analysis in Group 3 is interpreted as an inherited individual of Archean age. Its large discordance value (+27%) indicates at least one episode of significant loss of radiogenic Pb, which means the measured $^{207}Pb/^{206}Pb$ date is a minimum age for zircon crystallisation.

The uncertainty in the weighted mean $^{238}U/^{206}Pb$ age for Group 1 quoted above includes a component arising from the session-specific calibration uncertainty as determined on the $^{238}U/^{206}Pb$ reference zircon (in this case, 0.30% (2σ) on TEMORA2 in session 130036). However, this calibration uncertainty should be neglected when comparing weighted mean $^{238}U/^{206}Pb$ ages determined during the same analytical session, because that component of the 95% confidence interval is common to each weighted mean from that session. Consequently, the discussion below shows (in square brackets) narrowed 95% confidence intervals specific to weighted mean $^{238}U/^{206}Pb$ ages determined from session 130036, for the sole purpose of intra-session comparisons.

In comparison with other new SHRIMP zircon $^{238}U/^{206}Pb$ magmatic crystallisation ages presented in this Record, the 377.1 ± [1.5]1.8 Ma Royal George Granite is indistinguishable from the 379.3 ± [1.6]1.9 Ma Hazards Granite. It is distinguishably older than the 372.2 ± [1.6]1.9 Ma Meredith Granite, and is distinguishably younger than the 381.7 ± [1.8]2.2 Ma Gipps Creek Granite, the 392.2 ± [1.5]1.9 Ma Mount Stronach Granite, and the 393.3 ± [1.6]2.0 Ma Lisle Granodiorite.

2.3.5. Discussion

The previously undated S-type Royal George Granite intrudes the Mathinna Supergroup and is associated with significant greisen-style tin mineralisation at Royal George. It has been grouped with two other fractionated granites, the S-type Gipps Creek and the I-type Henbury Granites, as the Ben Lomond Batholith (see 2.4.1).

The magmatic crystallisation age of 377.1 ± 1.8 Ma for this sample is 4–5 Myr younger than the other S-type component of the Ben Lomond Batholith, the Gipps Creek Granite (see below). This is consistent with their spatial separation and subtle chemical differences that suggest they are separate intrusions. The age is indistinguishable from an existing SHRIMP zircon $^{238}U/^{206}Pb$ age of 376.7 ± 2.7 Ma from a sample of the Henbury Granite, which however is an I-type (Black et al., 2005; see Figure 1.3).

The 377.1 ± 1.8 Ma Royal George Granite is also indistinguishable from an existing SHRIMP zircon $^{238}U/^{206}Pb$ age of 377.8 ± 2.4 Ma for the chemically similar Lottah Granite (Black et al., 2005), which forms part of the Blue Tier Batholith to the north.

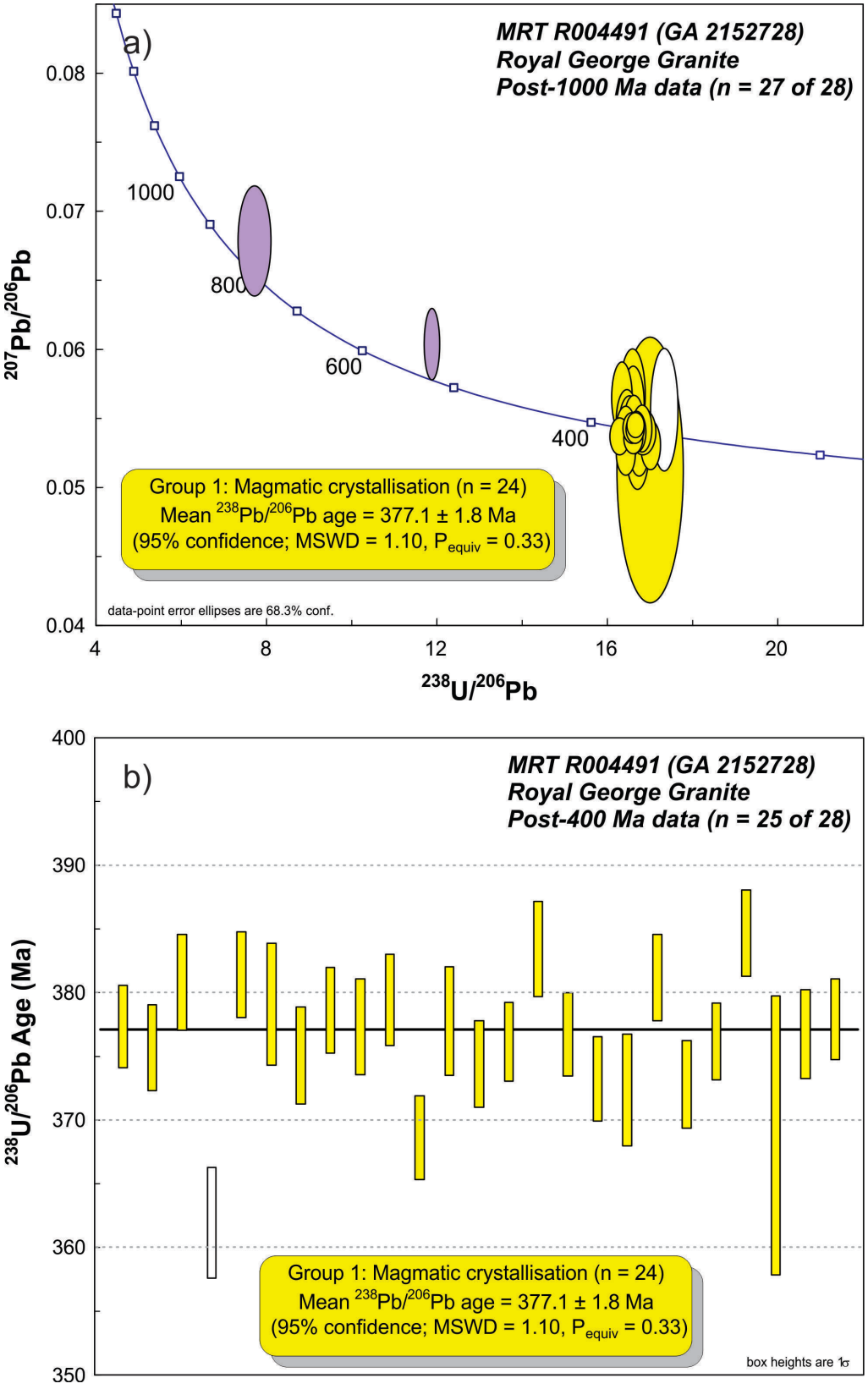

Figure 2.6 *SHRIMP U–Pb data for zircons from the Royal George Granite (MRT R004491, GA 2152728). (a) Tera-Wasserburg concordia diagram of post-1000 Ma data (Group 3 inherited individual not shown); (b) Post-400 Ma $^{238}U/^{206}Pb$ ages in order of acquisition. Yellow fill denotes Group 1 (magmatic crystallisation); purple fill denotes Group 2 (inheritance); white fill denotes excluded analysis (instrumental instability). Heavy black line: weighted mean $^{238}U/^{206}Pb$ age.*

Table 2.6 *SHRIMP U–Pb zircon data from Royal George Granite (MRT R004491, GA 2152728).*

Grain.area .replicate	$^{206}Pb_c$ (%)	U (ppm)	Th (ppm)	$^{232}Th/^{238}U$	$^{238}U/^{206}Pb$	± 1σ (%)	$^{207}Pb/^{206}Pb$	± 1σ (%)	$^{238}U/^{206}Pb$ Age (Ma)	± 1σ (Ma)	disc (%)
Group 3: Archean inherited individual $^{207}Pb/^{206}Pb$ age tabulated (n = 1)											
14.2.1	-0.07	78	89	1.17	2.475	1.42	0.20300	0.71	2850.5	11.6	+27
Group 2: Neoproterozoic-Cambrian inherited individuals (n = 2)											
20.2.1	0.27	87	49	0.59	7.658	3.33	0.06777	3.92	791.2	24.8	+9
13.2.1	0.13	281	89	0.33	11.851	1.04	0.06023	2.85	522.2	5.2	+15
Group 1: magmatic crystallisation (n = 24)											
1.1.1	0.05	636	99	0.16	16.590	0.89	0.05336	1.38	377.3	3.3	-10
2.1.1	0.15	515	94	0.19	16.665	0.93	0.05384	1.84	375.7	3.4	-3
3.1.1	-0.02	308	142	0.48	16.434	1.02	0.05467	2.70	380.8	3.8	+5
5.1.1	0.18	546	105	0.20	16.407	0.91	0.05222	1.95	381.4	3.4	-30
6.1.1	0.13	336	73	0.22	16.510	1.31	0.05404	2.85	379.1	4.8	-2
7.1.1	0.27	269	51	0.20	16.693	1.05	0.05250	3.61	375.1	3.8	-23
8.1.1	0.14	440	157	0.37	16.532	0.92	0.05351	1.92	378.6	3.4	-8
9.1.1	-0.09	252	51	0.21	16.591	1.03	0.05587	3.21	377.3	3.8	+16
10.1.1	0.03	311	76	0.25	16.495	0.98	0.05444	2.46	379.4	3.6	+3
11.1.1	0.07	435	83	0.20	16.994	0.92	0.05286	2.24	368.6	3.3	-15
12.1.1	-0.27	158	99	0.65	16.570	1.16	0.05652	3.89	377.8	4.3	+21
13.1.1	0.15	362	76	0.22	16.724	0.94	0.05248	2.38	374.4	3.4	-23
14.1.1	0.15	742	90	0.12	16.643	0.85	0.05404	1.27	376.1	3.1	-1
17.1.1	-0.02	257	84	0.34	16.317	1.01	0.05632	3.05	383.4	3.7	+18
18.1.1	0.12	464	78	0.17	16.618	0.90	0.05473	2.12	376.7	3.3	+6
19.1.1	0.03	404	121	0.31	16.777	0.92	0.05355	2.54	373.2	3.3	-6
20.1.1	0.15	394	86	0.22	16.819	1.22	0.05383	2.06	372.3	4.4	-2
21.1.1	0.04	421	152	0.37	16.416	0.92	0.05404	2.02	381.2	3.4	-2
22.1.1	0.05	323	328	1.05	16.798	0.95	0.05407	2.08	372.8	3.5	+0
23.1.1	0.17	987	87	0.09	16.642	0.83	0.05432	1.12	376.2	3.0	+2
24.1.1	0.10	425	118	0.29	16.263	0.91	0.05347	1.66	384.7	3.4	-11
25.1.1	0.66	61	39	0.66	16.986	3.07	0.05104	12.54	368.8	11.0	-53
26.1.1	0.18	346	97	0.29	16.616	0.96	0.05314	2.62	376.7	3.5	-13
16.2.1	-0.01	628	115	0.19	16.563	0.87	0.05410	1.36	377.9	3.2	-1
Not considered: instrument instability (n = 1)											
4.1.1	0.09	172	79	0.48	17.319	1.23	0.05546	5.33	361.9	4.3	+16

2.4. Gipps Creek Granite

Table 2.7 *Summary of results: Gipps Creek Granite (MRT R004493, GA 1951009).*

GA SampleNo	1951009
MRT Registration No	R004493
MRT Field No	SG36
Lithology	Alkali feldspar granite
Stratigraphic Unit	Gipps Creek Granite
Collector	JL Everard
Province/Region	Eastern Tasmanian Terrane
1:250 000 Sheet	LAUNCESTON (SK55-4)
1:100 000 Sheet	ST PAULS (8414)
Location (MGA94)	Zone 55, 556532 mE, 5385183 mN
Analytical Session	130036 (see Appendix Table A.1 for parameters derived from concurrent measurements of $^{238}U/^{206}Pb$ and $^{207}Pb/^{206}Pb$ reference zircons)
Interpreted Age	381.7 ± 2.2 Ma (95% confidence; 25 analyses of 25 zircons)
Geological Attribution	Magmatic crystallisation
Isotopic Ratio(s) Used	$^{238}U/^{206}Pb$ (^{204}Pb-corrected)

2.4.1. Location details and lithological characteristics

This sample was collected in 2001 using explosives, from large bedrock outcrops on the left bank of Buffalo Brook, about 40 m upstream of the bridge on Gipps Creek Road, about 6 km west-southwest of Rossarden, central eastern Tasmania (Figure 1.1). The sample is a coarse-grained equigranular-seriate white biotite granite with sparse to rare tabular K-feldspar phenocrysts (to 60 x 15 mm). Some cream to brown discoloration of feldspar and orange ferruginous alteration occurs along well-spaced joints, and the outcrop also contains aphyric microgranite dykes.

In thin section the rock consists mainly of slightly turbid K feldspar microperthite, clear to slightly turbid plagioclase (to ~An_{10}) and quartz, with common biotite (α nearly colourless, β and γ reddish-brown) and ragged anhedral muscovite, minor anhedral tourmaline and accessory topaz. Biotite contains abundant zircon inclusions, and some has been altered to chlorite.

Chemically (Table 1.2) it is a moderately fractionated peraluminous S-type granite.

2.4.2. Zircon description

Zircons from this sample range from euhedral to subhedral and rounded varieties, with external morphologies ranging from anhedral grains, through euhedral prisms with pyramidal terminations to elongate crystals (Figure 2.7). Aspect ratios range between 1:1 and 1:8 and long axes are ~60–500 µm. Grains are generally clear, colourless to light yellow in transmitted light.

In cathodoluminescence images, most grains are of moderate luminescence, although the full range extends from strong to weak. The majority of crystals display oscillatory zoning patterns, with more elongate crystals characterised by broader, mostly planar, banding parallel to the long axes. A few grains display sector zoning or no visible zoning. A number of crystals have very distinctive, often rounded cores, of either weak or strong luminescence, in most instances contrasting with oscillatory zoned rims.

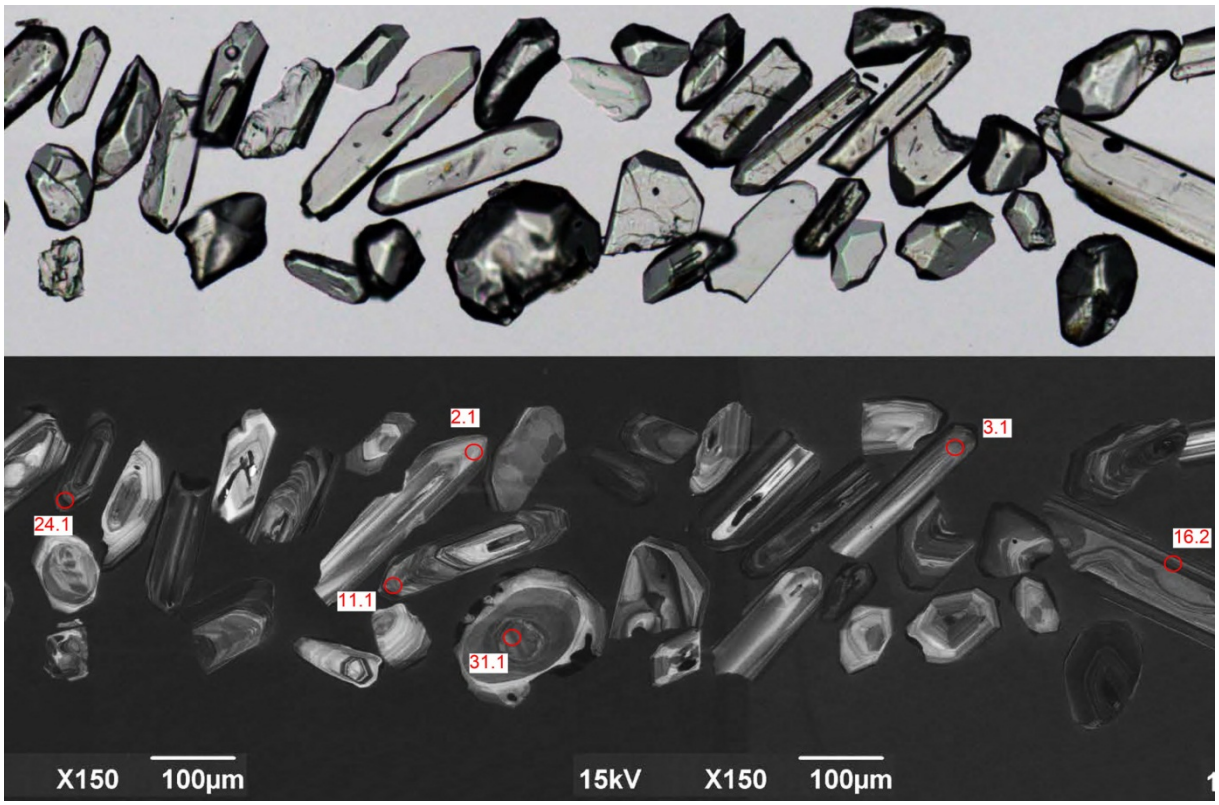

Figure 2.7 *Representative zircons from the Gipps Creek Granite (MRT R004493, GA 1951009). Transmitted light image is shown in the upper half; cathodoluminescence image in the lower half. SHRIMP analysis sites are labelled.*

2.4.3. U–Pb isotopic results

A total of 30 analyses were collected from 30 zircon crystals, the results of which are presented in Table 2.8 and Figure 2.8. The analysed zircons are characterised by low to moderate U contents (133–992 ppm, median = 322 ppm), and moderate Th/U (0.11–1.20, median = 0.36). Three analyses have excessively high $^{206}Pb_c$ (>3%). The data obtained from these three analyses are interpreted as unreliable and are not considered further.

The remaining 27 analyses have uniformly low $^{206}Pb_c$ (maximum 1.08%, median = 0.11%) and can be divided into two groups:

- Group 1 comprises 25 analyses of 25 zircons with individual $^{238}U/^{206}Pb$ ages between c. 389 Ma and c. 371 Ma, which yield a weighted mean age of 381.7 ± 2.2 Ma (MSWD = 1.3), and
- Group 2 comprises two analyses from two grains with individual $^{238}U/^{206}Pb$ ages of 613 ± 19 Ma (1σ) and 679 ± 13 Ma (1σ).

2.4.4. Geochronological interpretation

The weighted mean $^{238}U/^{206}Pb$ age of 381.7 ± 2.2 Ma, for the 25 analyses in Group 1, is interpreted as the best estimate of the age of magmatic crystallisation of the Gipps Creek Granite. The two analyses, 613 ± 19 Ma (1σ) and 679 ± 13 Ma (1σ) in Group 2, are interpreted as inherited individuals of Neoproterozoic age.

The uncertainty in the weighted mean $^{238}U/^{206}Pb$ age for Group 1 quoted above includes a component arising from the session-specific calibration uncertainty as determined on the $^{238}U/^{206}Pb$ reference zircon (in this case, 0.30% (2σ) on TEMORA2 in session 130036). However, this calibration uncertainty should be neglected when comparing weighted mean $^{238}U/^{206}Pb$ ages determined during the same analytical session, because that component of the 95% confidence interval is common to each weighted mean from that session. Consequently, the discussion below shows (in square brackets) narrowed 95% confidence intervals specific to weighted mean $^{238}U/^{206}Pb$ ages determined from session 130036, for the sole purpose of intra-session comparisons.

In comparison with other new SHRIMP zircon $^{238}U/^{206}Pb$ magmatic crystallisation ages presented in this Record, the 381.7 ± [1.8]2.2 Ma Gipps Creek Granite is indistinguishable from the 379.3 ± [1.6]1.9 Ma Hazards Granite. It is distinguishably older than the 372.2 ± [1.6]1.9 Ma Meredith Granite, and the 377.1 ± [1.5]1.8 Ma Royal George Granite and distinguishably younger than the 392.2 ± [1.5]1.9 Ma Mount Stronach Granite and 393.3 ± [1.6]2.0 Ma Lisle Granodiorite.

2.4.5. Discussion

In the Avoca-Rossarden area, the previously recognised ‘Ben Lomond Granite’ has been subdivided into the Henbury Granite and Gipps Creek Granite, mainly on the basis of geochemistry (e.g. Everard, 2005). The Gipps Creek Granite is characterised by lower CaO, higher ASI (i.e. is more peraluminous), lower Ce, Y, Th, Zr and Pb and higher P_2O_5 than the Henbury Granite. These differences suggest that the Gipps Creek Granite is a fractionated S-type, whereas the Henbury Granite is a fractionated I-type (cf. Chappell and White, 1992, p. 20-22). Both bodies display a range of textures and are associated with important mineralisation, notably Sn-W mineralisation at Aberfoyle and Storeys Creek.

The Henbury and Gipps Creek Granites can be distinguished from airborne radiometrics due to their differing thorium content, but their contact is difficult to identify in the field. Generally, but not invariably, surface samples of the Henbury Granite are characterised by a pink discoloration of potash feldspar, which does not extend to depth. The magmatic crystallisation age of 381.7 ± 2.2 Ma for the Gipps Creek Granite is distinguishably older than an existing SHRIMP zircon $^{238}U/^{206}Pb$ age of 376.7 ± 2.7 Ma for the Henbury Granite (Figure 1.3; Black et al., 2005). This confirms that the Gipps Creek Granite is a separate, earlier intrusion, not merely a local variant of the Henbury Granite. Both these ages are much older than a K–Ar muscovite age of 352 Ma and Rb–Sr whole rock, K-feldspar and plagioclase isochron ages of ~365 Ma for a sample of the ‘Ben Lomond Granite’ (McDougall and Leggo, 1965). That sample was probably from the Gipps Creek Granite, but in any case the K–Ar and Rb–Sr ages have very likely been affected by resetting (Black et al., 2005).

The Gipps Creek Granite has chemical similarities to the Lottah Granite of the Blue Tier Batholith (Black et al., 2005), although the 381.7 ± 2.2 Ma Gipps Creek Granite is distinguishably older than the existing SHRIMP zircon $^{238}U/^{206}Pb$ age of 377.8 ± 2.4 Ma for the Lottah Granite (Black et al., 2005; see Figure 1.3).

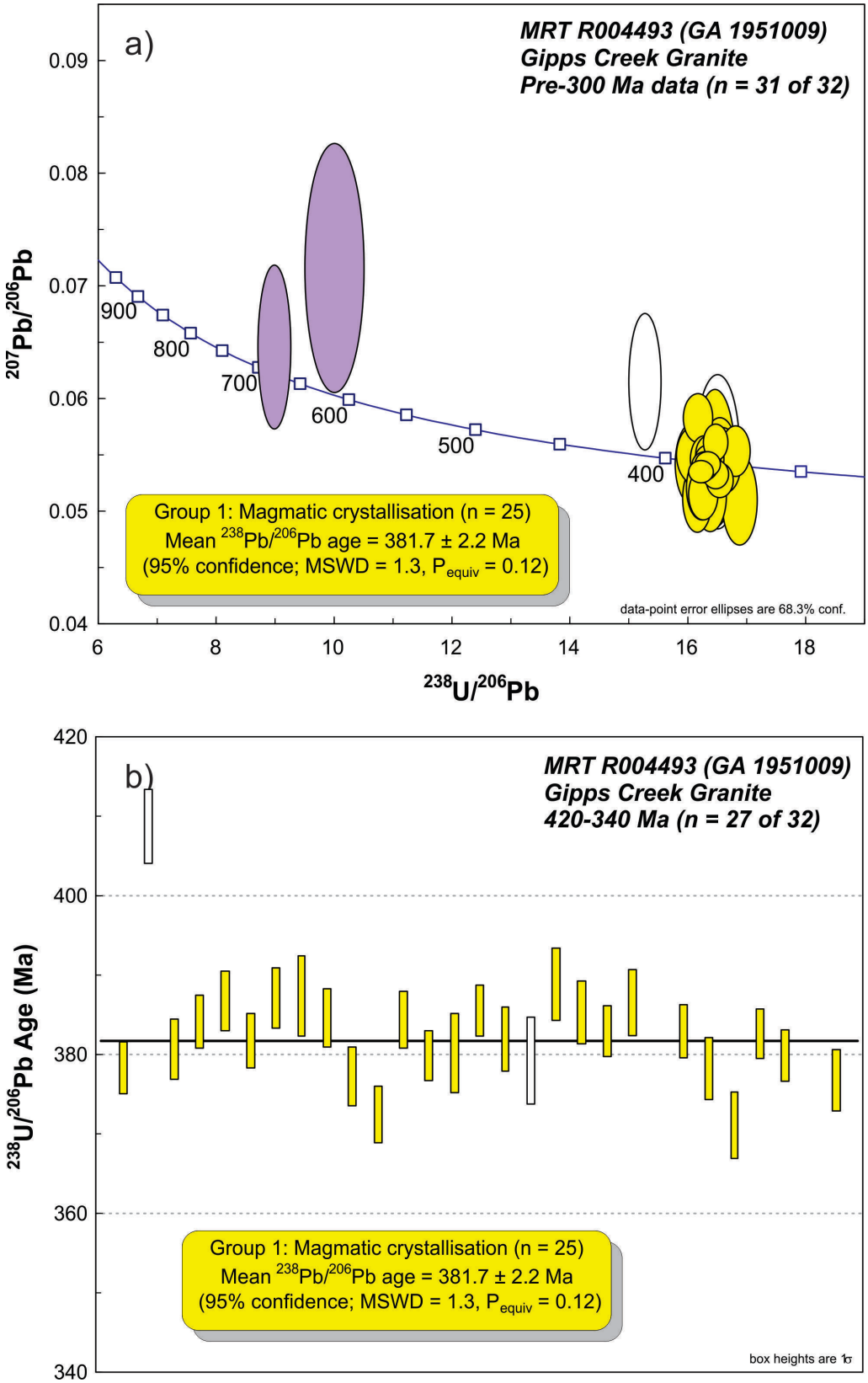

Figure 2.8 *SHRIMP U–Pb data for zircons from the Gipps Creek Granite (MRT R004493, GA 1951009). (a) Tera-Wasserburg concordia diagram of pre-300 Ma data (analysis 24.1.1 not shown); (b) 420-340 Ma $^{238}U/^{206}Pb$ ages in order of acquisition. Yellow fill denotes Group 1 (magmatic crystallisation); purple fill denotes Group 2 (inheritance); white fill denotes relatively high common Pb ($^{206}Pb_c$ >3%). Heavy black line: weighted mean $^{238}U/^{206}Pb$ age.*

Table 2.8 *SHRIMP U–Pb zircon data from Gipps Creek Granite (MRT R004493, GA 1951009).*

Grain.area .replicate	$^{206}Pb_c$ (%)	U (ppm)	Th (ppm)	$^{232}Th/^{238}U$	$^{238}U/^{206}Pb$	± 1σ (%)	$^{207}Pb/^{206}Pb$	± 1σ (%)	$^{238}U/^{206}Pb$ Age (Ma)	± 1σ (Ma)	disc (%)
Group 2: inherited individuals (n = 2)											
29.1.1	0.11	133	29	0.22	9.008	2.07	0.06456	7.44	678.6	13.3	+11
31.1.1	0.44	329	154	0.48	10.020	3.31	0.07160	10.22	613.2	19.3	+39
Group 1: magmatic crystallisation (n = 25)											
1.1.1	0.15	647	223	0.36	16.549	0.89	0.05268	1.94	378.2	3.3	-21
3.1.1	0.34	328	173	0.54	16.443	1.03	0.05391	3.01	380.6	3.8	-4
4.1.1	0.02	614	188	0.32	16.289	0.89	0.05397	1.55	384.1	3.3	-4
5.1.1	-0.35	332	67	0.21	16.175	1.00	0.05822	2.47	386.7	3.8	+29
6.1.1	0.12	496	170	0.35	16.393	0.93	0.05462	1.96	381.7	3.4	+4
7.1.1	0.32	312	177	0.58	16.159	1.01	0.05107	3.87	387.1	3.8	-60
8.1.1	-0.09	255	111	0.45	16.148	1.35	0.05496	3.17	387.3	5.1	+6
9.1.1	0.20	306	355	1.20	16.268	0.99	0.05147	2.92	384.6	3.7	-48
10.1.1	-0.09	260	132	0.52	16.595	1.02	0.05477	3.15	377.2	3.7	+7
11.1.1	-0.16	316	113	0.37	16.817	0.98	0.05527	2.70	372.4	3.5	+12
12.1.1	-0.02	362	170	0.49	16.278	0.95	0.05455	2.54	384.3	3.6	+2
13.1.1	1.08	793	176	0.23	16.478	0.85	0.05609	1.89	379.8	3.1	+17
14.1.1	0.02	106	45	0.44	16.462	1.35	0.05464	7.40	380.2	5.0	+5
17.1.1	0.07	683	182	0.28	16.228	0.85	0.05347	1.21	385.5	3.2	-11
18.1.1	0.30	192	69	0.37	16.386	1.09	0.05128	4.07	381.9	4.0	-52
20.1.1	-0.04	132	58	0.45	16.085	1.21	0.05414	4.46	388.8	4.6	-3
21.1.1	0.42	221	142	0.66	16.238	1.05	0.05201	3.61	385.3	3.9	-36
22.1.1	0.02	650	138	0.22	16.341	0.86	0.05413	1.34	382.9	3.2	-2
23.1.1	-0.13	174	100	0.60	16.183	1.11	0.05433	3.48	386.5	4.2	-0
16.2.1	0.02	466	100	0.22	16.340	0.90	0.05424	1.96	382.9	3.4	-1
25.1.1	0.01	203	150	0.76	16.552	1.07	0.05550	3.29	378.2	3.9	+13
26.1.1	0.34	167	68	0.42	16.879	1.16	0.05095	5.23	371.0	4.2	-57
27.1.1	0.43	829	200	0.25	16.355	0.85	0.05501	2.00	382.6	3.1	+7
28.1.1	0.11	573	114	0.21	16.478	0.88	0.05321	1.60	379.8	3.3	-13
30.1.1	0.01	212	125	0.61	16.619	1.06	0.05390	2.84	376.7	3.9	-3
Not considered: high Pb_c (n = 3)											
2.1.1	3.69	257	88	0.36	15.277	1.18	0.06145	6.52	408.7	4.7	+39
19.1.1	10.59	263	82	0.32	16.506	1.49	0.05523	8.21	379.2	5.5	+10
24.1.1	19.74	992	102	0.11	27.359	1.83	0.06352	7.55	231.4	4.1	+69

2.5. The Hazards Granite

Table 2.9 *Summary of results: The Hazards Granite (MRT R004499, GA 1950975).*

GA SampleNo	1950975
MRT Registration No	R004499
MRT Field No	-
Lithology	red alkali feldspar granite
Stratigraphic Unit	The Hazards Granite
Collector	JL Everard
Province/Region	Eastern Tasmanian Terrane
1:250 000 Sheet	OATLANDS (SK55-6)
1:100 000 Sheet	FREYCINET (8513)
Location (MGA94)	Zone 55, 605442 mE 5333133 mN
Analytical Session	130036 (see Appendix Table A.1 for parameters derived from concurrent measurements of $^{238}U/^{206}Pb$ and $^{207}Pb/^{206}Pb$ reference zircons)
Interpreted Age	379.3 ± 1.9 Ma (95% confidence; 23 analyses of 13 zircons)
Geological Attribution	Magmatic crystallisation
Isotopic Ratio(s) Used	$^{238}U/^{206}Pb$ (^{204}Pb-corrected)

2.5.1. Location details and lithological characteristics

This sample was collected in 2001 from blocks left in a disused building stone quarry at The Fisheries, on the south shore of Coles Bay, Freycinet Peninsula (now in the Freycinet National Park) (Figure 1.1). The hand specimen is a red, medium-grained (mostly <15 mm), equigranular granite consisting mainly of red potash feldspar, plagioclase, smoky quartz and minor biotite. In thin section, the potash feldspar is microcline microperthite with very abundant minute (<1 μm) inclusions of (?) hematite, whereas the exsolved plagioclase is relatively clear. Plagioclase subhedra are less abundant than microcline, and are probably albite. Ragged biotite booklets (α pale yellow, β and γ dark brown to olive green) are partly altered to dark green chlorite. Traces of muscovite are present. Zircon and possibly other accessory minerals are mainly associated with biotite.

Major and trace element analyses (Table 1.2) show that it is a strongly fractionated, weakly peraluminous I-type granite, notable for its high Y, Pb, Th and U contents.

2.5.2. Zircon description

Zircons from this sample were sparse with only about 40 crystals recovered (Figure 2.9). Grains are predominantly euhedral to subhedral with fewer subhedral and anhedral grain fragments. In transmitted light grains range from colourless to brown, and most are mottled and some are opaque. Almost all grains are extensively fractured and contain numerous inclusions and cavities. Aspect ratios range between 1:2 and 1:5, with long axes ~80–350 μm.

Cathodoluminescence images reveal medium to low emission with oscillatory zoning and lesser planar and/or mottled banding parallel to the long axes of grains. Most of the darker crystals also feature low contrast poorly defined concentric zoning and banding consistent with damage to the crystal lattices during metamictisation/alteration. Some grains contain structureless internal zones of high cathodoluminescence emission, which are conformably surrounded by oscillatory-zoned overgrowths.

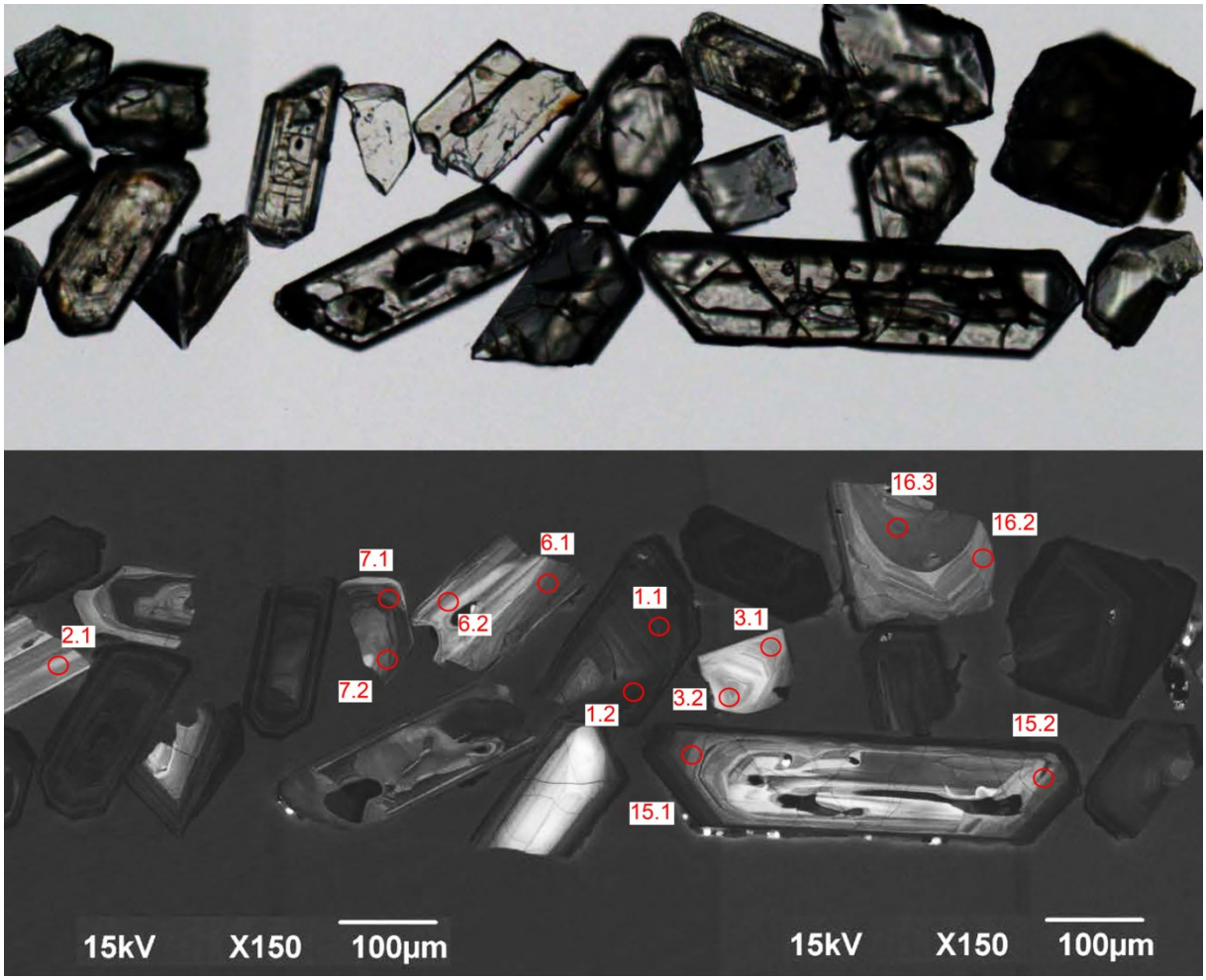

Figure 2.9 *Representative zircons from The Hazards Granite (MRT R004499, GA 1950975). Transmitted light image is shown in the upper half; cathodoluminescence image in the lower half. SHRIMP analysis sites are labelled.*

2.5.3. U–Pb isotopic results

A total of 32 analyses were collected from 19 zircon crystals, the results of which are presented in Table 2.10 and Figure 2.10. Twelve grains were analysed twice, and another grain three times. The analysed zircons are characterised by low to high U contents (112–5186 ppm, median = 423 ppm), and moderate Th/U (0.31–1.55, median = 0.52). Five analyses have excessively high $^{206}Pb_c$ (>1.7–55%). The data obtained from these 5 analyses are interpreted as unreliable and are not considered further. The remaining 24 analyses have reasonably low $^{206}Pb_c$ (maximum 0.71%) and can be divided into three groups:

- Group 1 comprises 23 analyses of 13 zircons with individual $^{238}U/^{206}Pb$ ages between c. 387 Ma and c. 370 Ma, which yield a weighted mean age of 379.3 ± 1.9 Ma (MSWD = 1.22);
- Group 2 is a single analysis with a $^{238}U/^{206}Pb$ age of 464 ± 4 Ma (1σ), and
- Group 3 comprises three analyses with individual $^{238}U/^{206}Pb$ ages of 236 ± 3 Ma, 295 ± 4 and 346 ± 3 Ma (1σ).

2.5.4. Geochronological interpretation

The weighted mean $^{238}U/^{206}Pb$ age of 379.3 ± 1.9 Ma, for the 23 analyses comprising Group 1, is interpreted as the best estimate of the age of magmatic crystallisation of The Hazards Granite. The Group 2 single analysis at 464 ± 4 Ma (1σ) is interpreted as an inherited individual of Ordovician age. Analyses comprising Group 3 are interpreted to have been affected by loss of radiogenic Pb during one or more events of unknown age, supported by a second analysis on grain 16 yielding an age which falls in Group 1.

The uncertainty in the weighted mean $^{238}U/^{206}Pb$ age for Group 1 quoted above includes a component arising from the session-specific calibration uncertainty as determined on the $^{238}U/^{206}Pb$ reference zircon (in this case, 0.30% (2σ) on TEMORA2 in session 130036). However, this calibration uncertainty should be neglected when comparing weighted mean $^{238}U/^{206}Pb$ ages determined during the same analytical session, because that component of the 95% confidence interval is common to each weighted mean from that session. Consequently, the discussion below shows (in square brackets) narrowed 95% confidence intervals specific to weighted mean $^{238}U/^{206}Pb$ ages determined from session 130036, for the sole purpose of intra-session comparisons.

In comparison with other new SHRIMP zircon $^{238}U/^{206}Pb$ magmatic crystallisation ages presented in this Record, the 379.3 ± [1.6]1.9 Ma Hazards Granite is indistinguishable from the 377.1 ± [1.5]1.8 Ma Royal George Granite and 381.7 ± [1.8]2.2 Ma Gipps Creek Granite. It is distinguishably older than the 372.2 ± [1.6]1.9 Ma Meredith Granite and distinguishably younger than the 392.2 ± [1.5]1.9 Ma Mount Stronach Granite and 393.3 ± [1.6]2.0 Ma Lisle Granodiorite. The age of The Hazards Granite is indistinguishable from that of the Bicheno Granite to the north (381.4 ± 2.7 Ma, Black et al., 2005; see Figure 1.3).

2.5.5. Discussion

Chappell et al. (1991) divided the granites of Freycinet Peninsula into four separate plutons, comprising from north to south, the Coles Bay, The Hazards, Freycinet and Schouten Island Granites. From their geochemistry (e.g. Rb, Sr and Ba contents), The Hazards Granite is the most fractionated and the Freycinet Granite the least. They are all similar fractionated I-types, grouped together by Everard (2001) and McClenaghan (2006) as the Freycinet Suite. However, as no contacts between these plutons have been defined, it seems possible that they are variably fractionated parts of the same large pluton.

Field relations clearly show that The Hazards Granite has intruded the more mafic Bluestone Bay Granodiorite at Wineglass Bay (Groves, 1965; Dunderdale, 1989). Similar relations have been demonstrated between the Coles Bay Granite and similar granodiorite west of Cape Tourville (Groves, 1965; Cocker, 1977) and the Freycinet Granite and granodiorite at Lagunta Creek (Everard, 2000). Age relationships between the Freycinet Suite and other eastern Tasmanian granites have not been

established, although the Coles Bay Granite crops out within 1–2 km of the S-type Bicheno Granite at the northern end of the Friendly Beaches.

McDougall and Leggo (1965) obtained a Rb–Sr minimum age of 368 Ma (this and following ages have been recalculated using the decay constants of Steiger and Jäger, 1977) from biotite from a 'leucocratic pink granite' collected from the same quarry sampled for this study. K–Ar dates from the same biotite yielded slightly younger ages of 353 to 361 (±10) Ma which were attributed to resetting. A whole rock-mineral Rb–Sr isochron gave a younger age of 345 Ma, which was discounted due to the likelihood of mobility of radiogenic Sr in feldspars.

Cocker (1977) also conducted a Rb–Sr study of granite and granodiorite in the Coles Bay - Bluestone Bay area. Probably the most reliable dates (recalculated using new decay constants) are from biotites: 370.8 ± 3 Ma from a pink felsic granite, and 372.8 ± 3 Ma from a granodiorite, both from north of Sleepy Bay.

Our new SHRIMP U–Pb zircon age of 379.3 ± 1.9 Ma is ~11 Myr older than the Rb–Sr biotite age from the same locality, and 8 Myr older that the Rb–Sr biotite age obtained from the similar Coles Bay Granite. This is broadly consistent with the observation of Black et al. (2005), that the SHRIMP ages from eastern Tasmanian granites are on average ~10 Myr older than Rb–Sr and K–Ar ages from the same body. They attributed this to 'residual heat associated with cooling of local magmas.'

The SHRIMP age is probably applicable to the other plutons of the Freycinet Suite and also places a minimum age constraint for the Bluestone Bay Granodiorite. The age relationship of the Freycinet Suite to the Bicheno Granite remains unresolved.

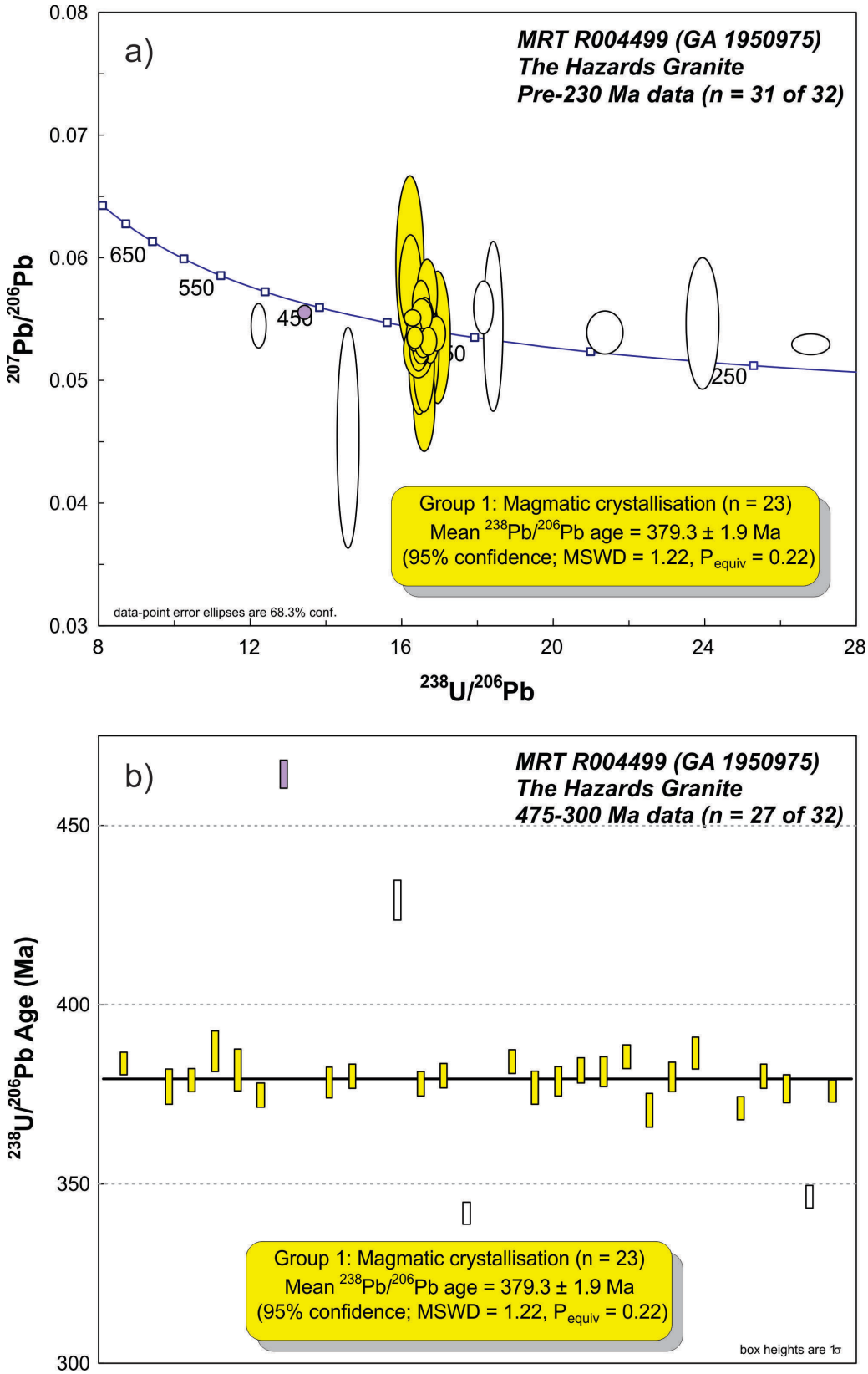

Figure 2.10 *SHRIMP U–Pb data for zircons from The Hazards Granite (MRT R004499, GA 1950975). (a) Tera-Wasserburg concordia diagram for pre-230 Ma data (analysis 14.2.1 not shown); (b) $^{238}U/^{206}Pb$ ages in order of acquisition. Yellow fill denotes Group 1 (magmatic crystallisation); purple fill denotes Group 2 (inheritance); white fill denotes relatively high common Pb ($^{206}Pb_c$ >1.7%) and Group 3 analyses affected by loss of radiogenic Pb. Heavy black line: weighted mean $^{238}U/^{206}Pb$ age.*

Table 2.10 *SHRIMP U–Pb zircon data from The Hazards Granite (MRT R004499, GA 1950975).*

Grain.area .replicate	$^{206}Pb_c$ (%)	U (ppm)	Th (ppm)	$^{232}Th/^{238}U$	$^{238}U/^{206}Pb$	± 1σ (%)	$^{207}Pb/^{206}Pb$	± 1σ (%)	$^{238}U/^{206}Pb$ Age (Ma)	± 1σ (Ma)	disc (%)
Group 2: inherited individual (n = 1)											
8.1.1	0.38	2067	658	0.33	13.389	0.88	0.05541	0.71	464.4	4.0	-9
Group 1: magmatic crystallisation (n = 23)											
1.1.1	0.12	1007	293	0.30	16.314	0.84	0.05331	1.10	383.5	3.1	-12
3.1.1	0.18	131	70	0.55	16.603	1.33	0.05250	6.15	377.0	4.9	-23
4.1.1	0.17	699	303	0.45	16.521	0.88	0.05288	1.49	378.9	3.2	-18
5.1.1	-0.40	92	86	0.97	16.166	1.53	0.05946	7.91	386.9	5.7	+35
6.1.1	0.12	264	104	0.41	16.394	1.57	0.05228	2.88	381.7	5.8	-29
7.1.1	0.25	529	214	0.42	16.711	0.93	0.05340	2.68	374.6	3.4	-9
10.1.1	0.82	160	62	0.40	16.553	1.16	0.04802	5.52	378.1	4.3	-285
11.1.1	0.10	428	222	0.54	16.471	0.92	0.05275	1.98	380.0	3.4	-20
14.1.1	0.05	376	187	0.52	16.569	0.93	0.05476	2.21	377.8	3.4	+6
15.1.1	0.18	391	195	0.52	16.465	0.93	0.05280	2.46	380.1	3.4	-19
11.2.1	0.27	552	215	0.40	16.288	0.89	0.05363	1.73	384.1	3.3	-8
10.2.1	0.24	127	62	0.50	16.615	1.26	0.05221	6.05	376.8	4.6	-29
2.2.1	0.71	178	154	0.89	16.537	1.13	0.05112	5.03	378.5	4.1	-55
7.2.1	0.06	341	139	0.42	16.400	0.96	0.05254	2.46	381.6	3.6	-24
6.2.1	0.50	169	113	0.69	16.417	1.14	0.05104	5.17	381.2	4.2	-59
1.2.1	0.34	1810	782	0.45	16.233	0.89	0.05495	0.83	385.4	3.3	+6
3.2.1	0.34	112	66	0.61	16.910	1.32	0.05337	6.71	370.4	4.7	-8
17.2.1	0.02	515	296	0.59	16.481	1.13	0.05514	1.68	379.7	4.1	+9
5.2.1	-0.48	152	94	0.64	16.189	1.18	0.05795	4.38	386.4	4.4	+28
20.1.1	0.09	460	141	0.32	16.880	0.91	0.05366	1.76	371.0	3.3	-4
15.2.1	-0.11	358	198	0.57	16.473	0.95	0.05609	2.28	379.9	3.5	+17
16.2.1	-0.30	209	102	0.51	16.631	1.07	0.05693	3.29	376.4	3.9	+24
21.1.1	0.10	726	278	0.39	16.658	0.86	0.05303	1.43	375.8	3.1	-14
Group 3: affected by loss of radiogenic Pb (n = 3)											
12.1.1	0.73	2523	485	0.20	26.802	1.21	0.05278	1.08	236.1	2.8	+27
19.1.1	0.11	523	486	0.96	21.343	1.48	0.05376	2.17	295.2	4.3	+19
16.3.1	0.74	417	325	0.80	18.123	0.92	0.05579	2.58	346.2	3.1	+23
Not considered: high Pb_c (n = 5)											
2.1.1	1.70	182	257	1.45	23.931	1.20	0.05449	6.55	263.9	3.1	+33
9.1.1	8.83	5186	1305	0.26	12.161	1.09	0.05430	2.22	509.4	5.3	-34
13.1.1	24.05	448	164	0.38	14.526	1.35	0.04510	13.24	429.2	5.6	+985
18.1.1	3.18	490	273	0.58	18.377	0.93	0.05426	8.50	341.6	3.1	+11
14.2.1	54.50	1618	1012	0.65	31.048	25.54	0.06669	302.97	204.4	51.4	+77

3. Western Tasmania Terrane

3.1. Meredith Granite

Table 3.1 *Summary of results: Meredith Granite (MRT R017895, GA 2153031).*

GA SampleNo	2153031
MRT Registration No	R017895
MRT Field No	-
Lithology	alkali feldspar granite/syenogranite
Stratigraphic Unit	Meredith Granite
Collector	Venture Minerals
Province/Region	Western Tasmanian Terrane
1:250 000 Sheet	BURNIE (SK55-3)
1:100 000 Sheet	PIEMAN (7914)
Location (MGA94)	Zone 55, 364258 mE 5386705 mN
Analytical Session	130036 (see Appendix Table A.1 for parameters derived from concurrent measurements of $^{238}U/^{206}Pb$ and $^{207}Pb/^{206}Pb$ reference zircons)
Interpreted Age	372.2 ± 1.9 Ma (95% confidence; 22 analyses of 22 zircons)
Geological Attribution	Magmatic crystallisation
Isotopic Ratio(s) Used	$^{238}U/^{206}Pb$ (^{204}Pb-corrected)

3.1.1. Location details and lithological characteristics

Venture Minerals provided a sample of the Meredith Granite from drillhole BW013 (down hole depth 339–347 m, RL 179 m), at the Big Wilson prospect, located about 3.8 km northeast of Parsons Hood and 16 km north-northwest of Renison Bell (Figure 1.2). Locally the granite intrudes the Wilson River Ultramafic Complex (Early Cambrian) and an east-facing sequence of Gordon Limestone (Ordovician) and Crotty Quartzite (Silurian).

The sample is a white coarse-grained equigranular biotite granite with minor pale green pinite alteration. The thin section consists mainly of quartz, potash feldspar, plagioclase and biotite. Potash feldspar (microcline microperthite) is slightly turbid due to minute inclusions. Plagioclase grains are generally small, euhedral and zoned with sericitised cores and clear albite rims. Small patches of micrographically intergrown fine-grained potash feldspar and quartz are present. Booklets of biotite (to 2 mm) are pleochroic (α pale orange-brown, β and γ very dark brownish-red) with numerous radiation haloes around small monazite and zircon inclusions. Minor secondary muscovite and pale green to brown chlorite are also present.

3.1.2. Zircon description

Zircons from this sample are predominantly euhedral to subhedral with external morphologies ranging from prismatic to elongate (Figure 3.1). Aspect ratios range from 1:1 to 1:6 and long axes are ~70–350 µm. In transmitted light the zircons are predominantly transparent, clear to colourless to faint yellow in colour. Cathodoluminescence images reveal relatively uniform moderate to high emission intensity but generally low contrast. Fine-scale concentric oscillatory zoning is best developed in equant grains, with elongate crystals generally characterised by broader banding parallel to their long axes. Rare grains contain central regions with bright structureless cores, overgrown by the high intensity low contrast zircon characteristic of the remainder of the population. These central regions are interpreted as inherited cores with magmatic overgrowths.

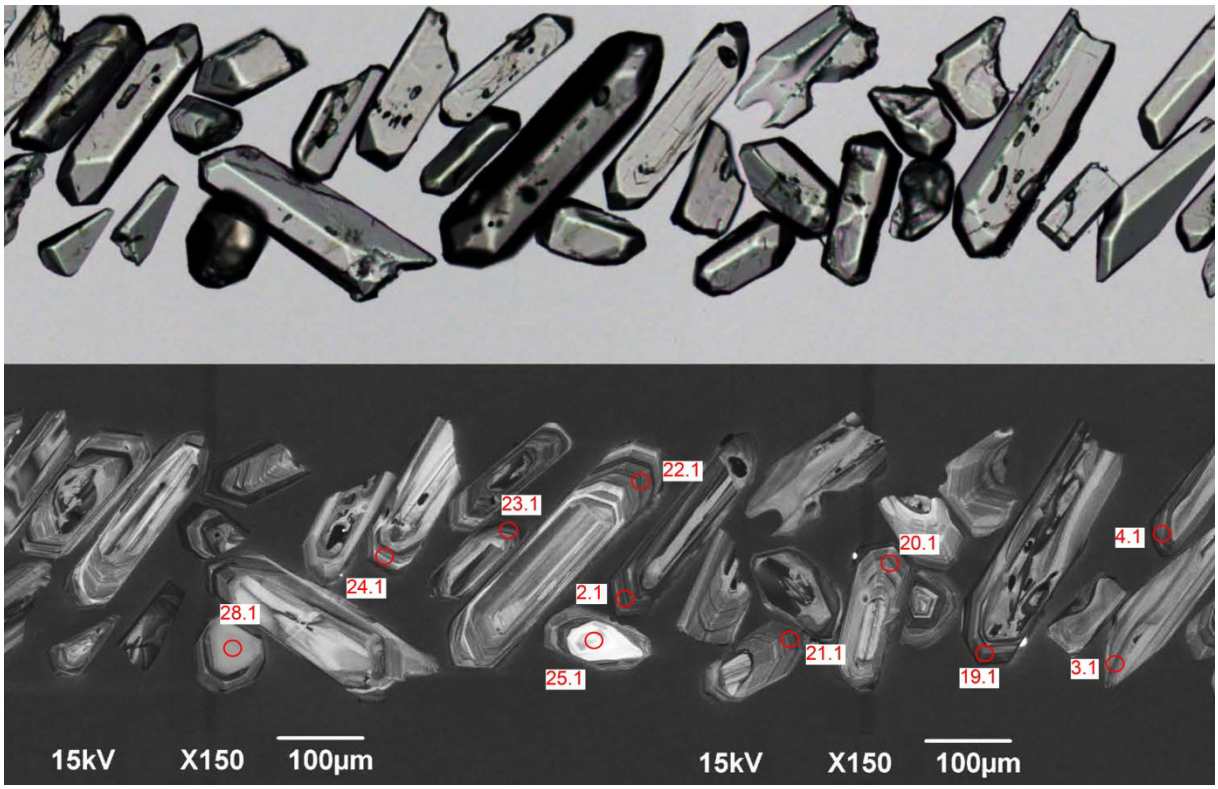

Figure 3.1 *Representative zircons from the Meredith Granite (MRT R017895, GA 2153031). Transmitted light image is shown in the upper half; cathodoluminescence image in the lower half. SHRIMP analysis sites are labelled.*

3.1.3. U–Pb isotopic results

A total of 26 analyses were collected from 26 zircon crystals, the results of which are presented in Table 3.2 and Figure 3.2. The analysed zircons are characterised by low to moderate U contents (43–623 ppm, median = 346 ppm), moderate Th/U (0.25–1.01, median = 0.38) and uniformly low $^{206}Pb_c$ (maximum 0.28%).

They can be divided into two groups:

- Group 1 comprises 22 analyses of 22 zircons with individual $^{238}U/^{206}Pb$ ages between c. 378 Ma and c. 368 Ma, which yield a weighted mean age of 372.2 ± 1.9 Ma (MSWD = 0.87), and

- Group 2 comprises four analyses with $^{207}Pb/^{206}Pb$ ages between c. 1432 Ma and c. 2035 Ma.

3.1.4. Geochronological interpretation

The weighted mean $^{238}U/^{206}Pb$ age of 372.2 ± 1.9 Ma, for the 22 analyses comprising Group 1, is interpreted as the age of magmatic crystallisation of the Meredith Granite. The four analyses in Group 2 are interpreted as inherited individuals of Meso- to Paleoproterozoic age.

The uncertainty in the weighted mean $^{238}U/^{206}Pb$ age for Group 1 quoted above includes a component arising from the session-specific calibration uncertainty as determined on the $^{238}U/^{206}Pb$ reference zircon (in this case, 0.30% (2σ) on TEMORA2 in session 130036). However, this calibration uncertainty should be neglected when comparing weighted mean $^{238}U/^{206}Pb$ ages determined during the same analytical session, because that component of the 95% confidence interval is common to each weighted mean from that session. Consequently, the discussion below shows (in square brackets) narrowed 95% confidence intervals specific to weighted mean $^{238}U/^{206}Pb$ ages determined from session 130036, for the sole purpose of intra-session comparisons.

In comparison with other new SHRIMP zircon $^{238}U/^{206}Pb$ magmatic crystallisation ages presented in this Record, the 372.2 ± [1.6]1.9 Ma Meredith Granite is distinguishably younger than the 377.1 ± [1.5]1.8 Ma Royal George Granite, the 379.3 ± [1.6]1.9 Ma Hazards Granite, the 381.7 ± [1.8]2.2 Ma Gipps Creek Granite, the 392.2 ± [1.5]1.9 Ma Mount Stronach Granite and the 393.3 ± [1.6]2.0 Ma Lisle Granodiorite.

3.1.5. Discussion

The Meredith Granite is the largest (~225 km^2) exposed granite body in western Tasmania (Figure 1.2). Airborne radiometrics clearly distinguish it from the less felsic Wombat Flat Granite to the northeast, which has a larger exposure (~60 km^2) than was thought previously from reconnaissance surface mapping (e.g. Turner et al., 1991). The form of the contact suggests that the Meredith Granite is either older than, or coeval with, the Wombat Flat Granite. Together, the two bodies constitute the Meredith Batholith.

Much of the Meredith Granite is poorly known due to difficult access, but several textural types are present. McClenaghan (in Turner et al., 1991) described it as a very coarse-grained equigranular biotite granite with very abundant intrusions of fine- to coarse-grained porphyritic granite containing phenocrysts of quartz, K-feldspar and plagioclase; quartz tourmaline nodules are abundant. Sharples (in Turner, 1992) mapped three variants based on texture, grain-size and colour (grey, grey-white and pink) in a reconnaissance traverse of the southeastern part of the pluton.

Camacho (1987, and in McClenaghan et al., 1989, p. 254) subdivided the Meredith Granite into nine plutons, based on granitic textures, proportions of accessory minerals (e.g. the monazite/apatite ratio) and degree of development of tourmaline nodules. Contacts were air-photo interpreted from joint patterns and partly verified by helicopter-based field inspection. No clear geochemical differences between the plutons have been established (from relatively limited data) and most subsequent workers (e.g. Turner et al., 1991) have not adopted Camacho's subdivision. Our dated sample is, however, probably from Camacho's Whyte Pine Granite.

The Meredith Granite is a fractionated I-type alkali feldspar granite/syenogranite associated with significant tin mineralisation (e.g. the Mt Lindsay and Mt Ramsay prospects). Camacho (1987)

suggested that it was related to the Wombat Flat Granite by a process of crystal fractionation and mineralogical re-equilibration, and McClenaghan (2006) assigned both plutons to the Meredith Suite.

Previous biotite K–Ar, Rb–Sr and Ar–Ar ages (ca. 338.5–366 Ma; McDougall and Leggo, 1965; Brooks, 1966; Sawka et al., 1990; McClenaghan et al., 1989) purported to be from the 'Meredith Granite' or 'Meredith Batholith' are all actually from the Wombat Flat Granite.

The indistinguishable SHRIMP ages of the Meredith Granite (372.2 ± 1.9 Ma) and Wombat Flat Granite (373.2 ± 1.9 Ma, Black et al., 2005) are consistent with both field relations and a genetic relationship (Figure 1.3).

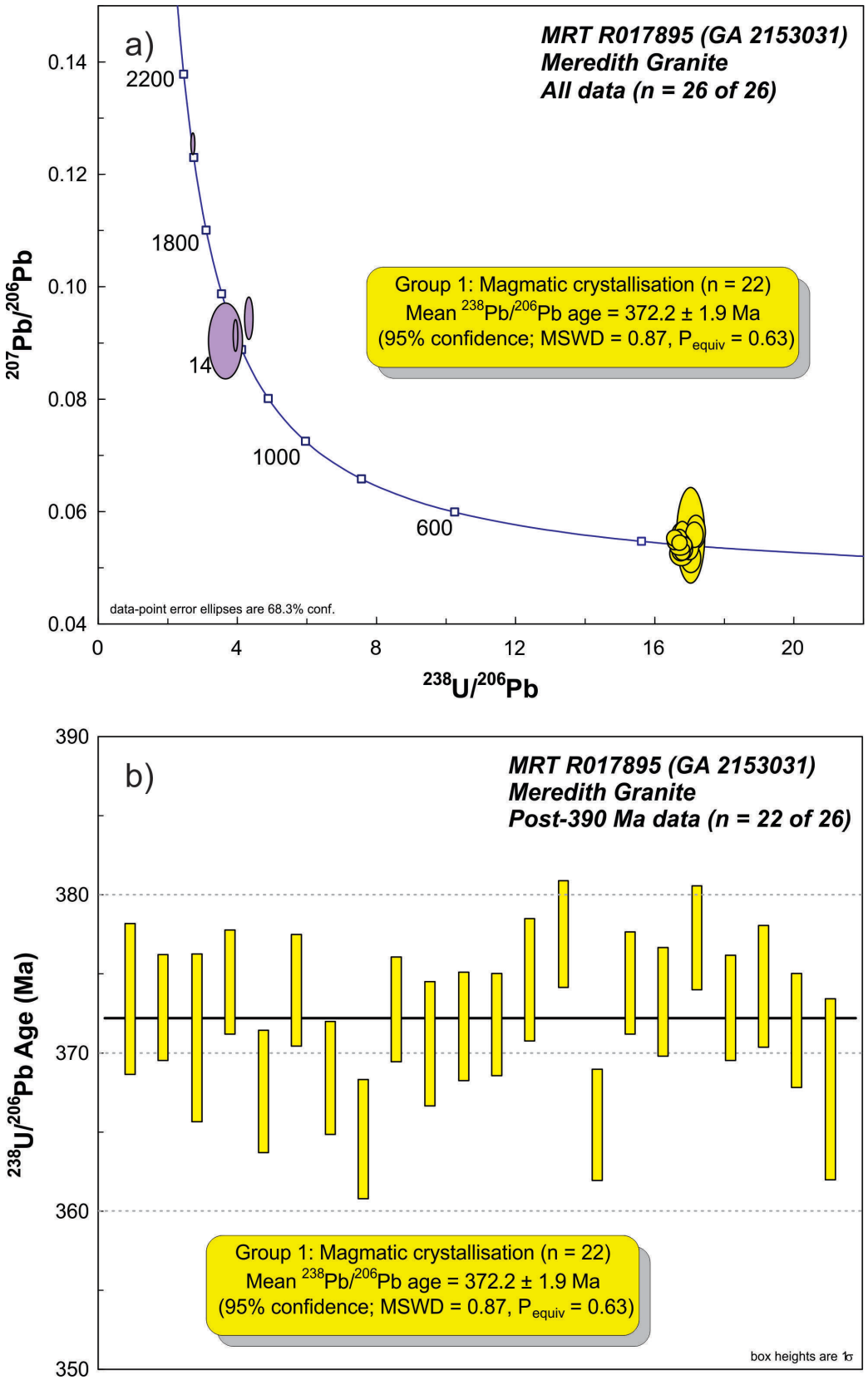

Figure 3.2 *SHRIMP U–Pb data for zircons from the Meredith Granite (MRT R017895, GA 2153031). (a) Tera-Wasserburg concordia diagram; (b) Post-390 Ma $^{238}U/^{206}Pb$ ages in order of acquisition. Yellow fill denotes Group 1 (magmatic crystallisation); purple fill denotes Group 2 (inheritance). Heavy black line: weighted mean $^{238}U/^{206}Pb$ age.*

Table 3.2 *SHRIMP U–Pb zircon data from Meredith Granite (MRT R017895, GA 2153031).*

Grain.area .replicate	$^{206}Pb_c$ (%)	U (ppm)	Th (ppm)	$^{232}Th/^{238}U$	$^{238}U/^{206}Pb$	± 1σ (%)	$^{207}Pb/^{206}Pb$	± 1σ (%)	$^{238}U/^{206}Pb$ Age (Ma)	± 1σ (Ma)	disc (%)
Group 2: inherited individuals $^{207}Pb/^{206}Pb$ ages tabulated (n = 4)											
29.1.1	0.14	132	64	0.50	2.746	1.18	0.12545	1.01	2035.2	17.8	+2
27.1.1	-0.04	43	38	0.91	4.362	1.88	0.09435	2.64	1515.1	49.9	+13
26.1.1	0.02	113	79	0.72	3.977	1.25	0.09128	2.01	1452.5	38.2	+0
28.1.1	-0.03	146	143	1.01	3.686	8.56	0.09029	4.96	1431.6	94.6	-9
Group 1: magmatic crystallisation (n = 22)											
1.1.1	0.27	354	107	0.31	16.768	1.32	0.05245	2.74	373.4	4.8	-23
2.1.1	-0.01	512	175	0.35	16.793	0.93	0.05421	2.15	372.9	3.4	+2
3.1.1	0.05	281	92	0.34	16.883	1.48	0.05449	2.99	370.9	5.3	+5
4.1.1	-0.13	554	114	0.21	16.719	0.91	0.05502	2.08	374.5	3.3	+10
5.1.1	0.28	246	121	0.51	17.044	1.08	0.05158	3.34	367.5	3.9	-39
6.1.1	0.14	376	166	0.46	16.743	0.97	0.05294	2.34	374.0	3.5	-15
7.1.1	0.16	296	139	0.48	17.004	1.00	0.05372	2.89	368.4	3.6	-3
8.1.1	-0.38	228	80	0.36	17.190	1.07	0.05629	3.46	364.5	3.8	+22
9.1.1	0.20	429	122	0.29	16.800	0.92	0.05285	2.06	372.7	3.3	-16
10.1.1	-0.03	192	46	0.25	16.901	1.10	0.05437	3.90	370.6	4.0	+4
11.1.1	0.15	346	137	0.41	16.850	0.96	0.05334	2.54	371.7	3.5	-8
12.1.1	0.14	508	157	0.32	16.844	0.89	0.05395	1.81	371.8	3.2	-1
13.1.1	-0.03	203	61	0.31	16.712	1.07	0.05446	4.05	374.6	3.9	+4
17.1.1	-0.16	403	147	0.38	16.580	0.92	0.05521	1.72	377.5	3.4	+11
18.1.1	-0.13	278	187	0.69	17.146	1.00	0.05575	2.64	365.4	3.5	+18
19.1.1	0.02	504	154	0.32	16.722	0.89	0.05432	1.66	374.4	3.2	+3
20.1.1	0.15	346	159	0.48	16.778	0.95	0.05384	2.32	373.2	3.4	-2
21.1.1	-0.03	474	148	0.32	16.591	0.90	0.05459	1.85	377.3	3.3	+5
22.1.1	-0.10	418	187	0.46	16.794	0.92	0.05575	2.82	372.9	3.3	+16
23.1.1	0.04	623	128	0.21	16.732	1.06	0.05325	1.50	374.2	3.9	-10
24.1.1	-0.02	258	112	0.45	16.862	1.00	0.05440	3.35	371.4	3.6	+4
25.1.1	-0.08	76	38	0.52	17.038	1.60	0.05566	10.12	367.7	5.7	+17

Acknowledgements

Jenny Stein and other staff at Venture Minerals kindly provided core of the Meredith Granite. The Tasmanian National Parks and Wildlife Service is thanked for issuing a sample permit to collect The Hazards Granite, and Mr R. Gee granted permission to collect the Royal George Granite sample from his property *Royslea*. At MRT, Shane Heawood assisted with sample collection and cut thin sections, Les Hay, Richie Woolley, Ken Gibbs and Jafar Taheri performed XRF analyses and Tony 'Al' Hollick prepared Figures 1.1 and 1.2. MRT's contribution to the cost of SHRIMP analyses was funded from the Western Tasmanian Geoscience Initiative.

The SHRIMP zircon U–Pb analytical program was conducted using high quality zircon separates, mounts, photographs and cathodoluminescence images professionally and skilfully prepared by David DiBugnara, Benjamin Linehan, and Rick Long of GA's Mineral Separation Laboratory. Patrick Burke (GA) provided valuable technical support and assistance in optimising analytical conditions on the SHRIMP IIe during data acquisition. Simon Bodorkos and Emma Chisholm (GA) are thanked for providing formal reviews of this Record.

References

Black, L.P., Kamo, S.L., Allen, C.M., Davis, D.W., Aleinikoff, J.N., Valley, J.W., Mundil, R., Campbell, I.H., Korsch, R.J., Williams, I.S. and Foudoulis, C. 2004. Improved $^{206}Pb/^{238}U$ microprobe geochronology by the monitoring of a trace element related matrix effect; SHRIMP, ID-TIMS, ELAICP-MS and oxygen isotope documentation for a series of zircon standards. Chemical Geology 205, 115–140.

Black, L.P., McClenaghan, M.P., Korsch, R.J., Everard, J.L. and Foudoulis, C. 2005. The significance of Devonian-Carboniferous igneous activity in Tasmania, as derived from U–Pb SHRIMP dating of zircon. Australian Journal of Earth Sciences 52, 807–829.

Black, L.P., Everard, J.L., McClenaghan, M.P., Korsch, R.J., Calver, C.R., Fioretti, A.M., Brown, A.V. and Foudoulis, C. 2010. Controls on Devonian–Carboniferous magmatism in Tasmania, based on inherited zircon age patterns, Sr, Nd and Pb isotopes, and major and trace element geochemistry. Australian Journal of Earth Sciences 57, 933–968.

Bottrill, R.S. 1996. Diamond drilling in the Lisle valley. Tasmanian Geological Survey Record 1996/04.

Brooks, C. 1966. The rubidium–strontium ages of some Tasmanian igneous rocks. Journal of the Geological Society of Australia 13, 457–469.

Brooks, C. and Compston, W. 1965. The age and initial Sr^{87}/Sr^{86} of the Heemskirk Granite, Western Tasmania. Journal of Geophysical Research 70, 6249–6262.

Camacho, A. 1987. Geochemistry of some fractionated western Tasmanian granites. M.Sc. thesis, La Trobe University, Melbourne. (unpubl.).

Carson, C.J., Hollis, J.A., Glass, L.M., Close, D.F., Whelan, J.A. and Wygralak, A. 2010. Summary of results. Joint NTGS-GA geochronology project: Arunta, Pine Creek regions July 2007–July 2009. Northern Territory Geological Survey, Record 2010-004.

Chappell, B.W., English, P.M., King, P.L., White, A.J.R. and Wyborn, D. 1991. Granites and related rocks of the Lachlan Fold Belt (1:2500000 scale map). Bureau of Mineral Resources, Geology and Geophysics, Canberra.

Chappell, B.W. and White, A.J.R. 1992. I- and S-type granites in the Lachlan Fold Belt. Transactions of the Royal Society of Edinburgh: Earth Sciences 83, 1–26.

Claoué-Long, J.C., Compston, W., Roberts, J. and Fanning, C.M. 1995. Two Carboniferous ages: a comparison of SHRIMP zircon dating with conventional zircon ages and $^{40}Ar/^{39}Ar$ analysis. In: Berggren, W.A., Kent, D.V., Aubry, M-P. and Hardenbol, J. (editors) Geochronology, time scales and global stratigraphic correlation. Society for Sedimentary Geology, Special Publication 54, 3–21.

Cocker, J.D. 1977. Petrogenesis of Tasmanian granitoids. PhD thesis, University of Tasmania (unpubl.).

Cocker, J.D. 1982. Rb–Sr geochronology and Sr isotopic composition of Devonian granitoids, eastern Tasmania. Journal of the Geological Society of Australia 29, 139–157.

Collins, W.J. 1996, S- and I-type granitoids of the eastern Lachlan fold belt: Products of three-component mixing: Royal Society of Edinburgh Transactions 88, 171–179.

Compston, W., Williams, I.S. and Meyer, C. 1984. U–Pb geochronology of zircons from lunar breccia 73217 using a sensitive high mass-resolution ion microprobe. Journal of Geophysical Research 89, Supplement B, 525–534.

Dunderdale, C. 1989. The granitoids of the Hazards Range, eastern central Tasmania: conditions of emplacement and alteration. B.Sc. thesis, University of St Andrews (Scotland).

Everard, J.L. 2001. Intrusive relationships of granite and dolerite at Lagunta Creek, Freycinet Peninsula. Papers and Proceedings of the Royal Society of Tasmania 135, 63–74.

Everard, J.L. (compiler) 2005. Tasmanian Granites and Associated Mineralisation (1:500 000 Scale Map). Mineral Resources Tasmania, Hobart and Geoscience Australia, Canberra.

Groves, D.I. 1965. Granites of the Coles Bay area. Technical Reports of the Department of Mines, Tasmania 10, 64–71.

Groves, D.I., Martin, E.L., Murchie, H. and Wellington, H.K. 1973. A century of tin mining at Mt Bischoff, 1871–1971. Geological Survey Tasmania Bulletin 54.

Jaffey, A.H., Flynn, K.F., Glendenin, L.E., Bentley, W.C. and Essling, A.M. 1971. Precision measurement of half-lives and specific activities of ^{235}U and ^{238}U. Physical Review C 4, 1889–1906.

Ludwig, K.R. 2003. User's manual for Isoplot 3.6: a geochronological toolkit for Microsoft Excel®. Berkeley Geochronology Center, Special Publication 4.

Ludwig, K.R. 2009. SQUID 2.50: A user's manual. Berkeley Geochronology Center, Special Publication 5.

Mackenzie, D. E., Black, L.P. and Sun, S-S. 1988. Origin of alkali feldspar granites: An example from the Poimena Granite, northeastern Tasmania, Australia. Geochimica et Cosmochimica Acta 52, 2507–2524.

McClenaghan, M.P., Camacho, A., Higgins, N.C. and Reid, E.J. 1989. Mid-Palaeozoic granitoids. In: Burrett C.F. and Martin E.L. (editors). Geology and Mineral Resources of Tasmania. Geological Society of Australia Special Publication 15, p. 253–270.

McClenaghan, M.P. (compiler). 1994a. Digital geological atlas 1: 25000 series. Sheet 5444. Scottsdale. Tasmanian Geological Survey.

McClenaghan, M.P. (compiler). 1994b. Digital geological atlas 1: 25000 series. Sheet 5443. Springfield. Tasmanian Geological Survey.

McClenaghan, M.P. 2006. The geochemistry of Tasmanian Devonian–Carboniferous granites and implications for the composition of their source rocks. Tasmanian Geological Survey Record 2006/06.

McClenaghan, M.P., Turner, N.J., Baillie, P.W., Brown, A.V., Williams, P.R. and Moore, W.R. 1982. Geology of the Ringarooma- Boobyalla area. Geological Survey Bulletin 61. Tasmania Department of Mines.

McDougall, I. and Leggo, P.J. 1965. Isotopic age determinations on granitic rocks from Tasmania. Journal of the Geological Society of Australia 12, 295–332.

Montgomery, A. 1994. Report on certain portions of the Lisle Goldfield. Unpublished Reports, Department of Mines Tasmania 1861–1920, 44–51.

Nasdala, L., Hofmeister, W., Norberg, N., Mattinson, J.M., Corfu, F., Dörr, W., Kamo, S.L., Kennedy, A.K., Kronz, A., Reiners, P.W., Frei, D., Kosler, J., Wan, Y., Götze, J., Häger, T., Kröner, A. and Valley, J.W. 2008. Zircon M257 – a homogeneous natural reference material for the ion microprobe U–Pb analysis of zircon. Geostandards and Geoanalytical Research 32, 247–265.

Nelson, D.R. 1997. Compilation of SHRIMP U–Pb zircon geochronology data, 1996. Geological Survey of Western Australia, Record 1997/2.

Reed, A.R. 2001. Pre-Tabberabberan deformation in eastern Tasmania: a southern extension of the Benambran Orogeny. Australian Journal of Earth Sciences 48, 785–796.

Reid, A.M. 1926. The Golconda mining district. Bulletin of the Geological Survey of Tasmania 37.

Roach, M. 1991. The regional geophysical setting of gold mineralisation in northeast Tasmania. Ph. D. thesis, University of Tasmania.

Roach, M.J. 1992. Geology and geophysics of the Lisle-Golconda goldfield. Geological Survey of Tasmania Bulletin 70, 189–198.

Robinson, K.P. 1982. The geology and geochemistry of the Mt Stronach region - Scottsdale. B.Sc. Hons. thesis, University of Tasmania (unpubl.).

Sawka, W.N., Heizler, M.T., Kistler, R.W. and Chappell, B.W. 1990. Geochemistry of highly fractionated I- and S-type granites from the tin-tungsten province of western Tasmania. Geological Society of America Special Paper 246, 161–179.

Seymour, D.B., Woolward, I.R., McClenaghan, M.P. and Bottrill, R.S. 2011. Stratigraphic revision and re-mapping of the Mathinna Supergroup between the River Tamar and the Scottsdale Batholith. Mineral Resources Tasmania 1: 25000 Scale Digital Geological Map Series, Explanatory Report 4.

Sircombe, K.N., Cassidy, K.F., Champion, D.C. and Tripp, G. 2007. Compilation of SHRIMP U–Pb geochronological data: Yilgarn Craton, Western Australia, 2004–2006. Geoscience Australia, Record 2007/01.

Stacey, J.S. and Kramers, J.D. 1975. Approximation of terrestrial lead isotope evolution using a two-stage model. Earth and Planetary Science Letters 26, 207–221.

Steiger, R.H. and Jäger, E. 1977. Subcommission on geochronology: convention on the use of decay constants in geo- and cosmochronology. Earth and Planetary Science Letters 36, 359–362.

Stern, R.A., Bodorkos, S., Kamo, S.L., Hickman, A.H. and Corfu, F. 2009. Measurement of SIMS instrument mass fractionation of Pb isotopes during zircon dating. Geostandards and Geoanalytical Research 33, 145–168.

Thureau, G. 1882. Report on the mineral resources and on the permanency of the Lisle goldfield. House of Assembly Paper Tasmania 1882 (46).

Tucker, R.D., Bradley, D.C., Ver Sraeten, C.A., Harris, A.G., Ebert, J.R. and McCutcheon, S.R. 1998. New U–Pb zircon ages and the duration and division of Devonian time. Earth and Planetary Science Letters 158, 175–186.

Turner, N.J., Black, L.P. and Higgins, N.C. 1986. The St Marys Porphyrite - a Devonian ash-flow tuff and its feeder. Australian Journal of Earth Sciences 33, 201–218.

Turner, N.J., Brown, A.V., McClenaghan, M.P. and Soetrisno, Ir. 1991. Geological Atlas 1:50,000 Series, sheet 43 (7914N): Corinna. Tasmania Department of Resources and Energy, Division of Mines and Mineral Resources.

Turner, N.J. (editor) 1992. Corinna 1:50 000 map: field guide to selected rock exposures. Tasmania Department of Mines Report 1992/06.

Twelvetrees, W.H. 1909. The Lisle Goldfield. Bulletin of the Geological Survey of Tasmania 4.

VandenBerg, A.H.M., Willman, C.E., Maher, S., Simons, B.A., Cayley, R.A., Taylor, D.H., Morand, V.J., Moore, D.H and Radojkovic, A. 2000 (editors) The Tasman Fold Belt in Victoria. Geological Survey of Victoria, Special Publication, Melbourne, 462 pp.

White, A.J R. and Chappell, B.W. 1977. Ultrametamorphism and granitoid genesis. Tectonophysics 43, 7–22.

Williams, E., McClenaghan, M.P., Collins, P.L.F., Brown, S.G., Camacho, A., Dronseika, E.V., Higgins, N.C., Morland, R., Reid, E.J. and Seymour, D.B. 1989. Mid-Paleozoic deformation, granitoids and ore deposits. In: Burrett, C.F. and Martin, E.L. (editors) Geology and mineral resources of Tasmania. Geological Society of Australia Special Publication 15, 238–292.

Williams, I.S., Buick, I.S. and Cartwright, I. 1996. An extended episode of early Mesoproterozoic metamorphic fluid flow in the Reynolds Range, central Australia. Journal of Metamorphic Geology 14, 29–47.

Williams, I.S. 1998. U–Th–Pb geochronology by ion microprobe. In: McKibben, M.A., Shanks III, W.C. and Ridley, W.I. (editors) Applications of microanalytical techniques to understanding mineralizing processes. Reviews in Economic Geology 7, 1–35.

Appendix A. SHRIMP Analytical Procedures

A.1. Analytical Procedures

All isotopic analyses reported in this Record were undertaken using the SHRIMP IIe at Geoscience Australia in Canberra. A summary of key parameters from the single analytical session is shown in Appendix Table A.1. The analytical procedures adopted (and outlined below) for zircon follow those published by Compston et al. (1984), Claoué-Long et al. (1995), Nelson (1997), and Williams (1998).

A.1.1. Sample acquisition and crushing

The Meredith Granite sample was collected at Venture Mineral's core shed at Tullah, and drill hole details were supplied by the company. The location of the sample of Lisle Granodiorite was recorded to within about 100 m, and those of the other field sites were determined using hand-held GPS units with accuracies of about 10 m. All are referred to the Geocentric Datum of Australia 1994 (GDA94). Co-ordinates are reported as decimal latitude and longitude, and as Map Grid of Australia eastings and northings (MGA94; Zone 55). Site locations are labelled using the relevant identifiers in each of the corporate databases: SampleID for MRT and FIELDSITES SampleNo for GA.

Samples were submitted to the Mineral Separation Laboratory at Geoscience Australia, where they were pulverised (to 2–5 cm pieces) using a pre-cleaned hydraulic splitter, ultrasonically washed in water, and dried under heat lamps. Samples were then crushed using a Rocklabs Boyd crusher, and milled using a Rocklabs continuous ring mill.

A.1.2. Mineral separation

Mineral-density separation was undertaken using a Wilfley table, with multiple iterations employed in order to successively deslime the rock flours and decant bulk low-density minerals such as quartz and feldspar, thereby reducing the sample to about 5% of its post-milling weight. Strongly paramagnetic grains were successively removed from this heavy fraction using a ferrous magnet and a rare-earth element magnet, before the remainder underwent a series of magnetic separations using a Frantz barrier separator. This typically involved 6–8 separations in total, with adjustments (firstly to the magnet current, and secondly to the horizontal tilt of the chute) aimed at the sequential removal of minerals with progressively weaker paramagnetism.

In cases where the initial Frantz separation (aimed at removing the most strongly paramagnetic material) demonstrated that the bulk of the heavy fraction was only weakly paramagnetic, the heavy fraction was immersed in liquid diiodomethane (specific gravity 3.3), in order to further reduce the low-density mineral content before the remaining Frantz separations were carried out. Where available, 300–400 zircons were hand-picked for each sample, commencing with grains in the least magnetic fraction, and progressing to successively more magnetic fractions in samples with low yield, without any discrimination based on the external morphologies of the grains.

A.1.3. Mount preparation

Hand-picked zircon separates were placed in rows on adhesive tape, along with a row of the $^{238}U/^{206}Pb$ reference zircon TEMORA2 (Black et al., 2004), a row of the $^{207}Pb/^{206}Pb$ reference zircon OG1 (Stern et al., 2009), and a fragment of the Sri Lankan gem zircon M257 (Nasdala et al., 2008) as a uranium concentration reference material. The grains were then mounted in a 25 mm-diameter epoxy disc, and once cured, the mount surface was polished using a series of successively finer diamond pastes, in order to expose longitudinal sections of the crystals. The grain-rows were photographed in transmitted light and reflected light using a Zeiss MC80 camera attached to a Zeiss Axioplan polarising microscope. The polished surface was then coated with a 20 Å thickness of high-purity (99.999%) gold, and cathodoluminescence (CL) images were acquired with the JEOL JSM-6490LV scanning electron microscope (SEM) at Geoscience Australia, using an accelerating voltage of 15 keV and a Robinson CL detector.

The gold coat was removed using an iodide solution, and the mount surface ultrasonically cleaned using ethanol, petroleum spirit and a 10% Extran solution, and triple-rinsed in quartz-distilled water, in order to minimise the amount of non-radiogenic Pb contamination on the polished surface prior to analysis. The mount was dried overnight in an oven at 30°C, then recoated with a 150 Å thickness of high-purity (99.999%) gold, to facilitate the establishment of a homogeneous electric potential across the surface during analysis, thereby avoiding charge buildup. Finally, the mount was loaded into the high-vacuum sample lock of the SHRIMP at least 12 hours prior to commencement of the analytical session, to facilitate degassing of any remaining volatile species, and to minimise the potential for hydride residues on the mount surface.

A.1.4. Instrument setup and data acquisition

A 30 µm-diameter primary beam of O_2^- ions at 10 keV, purified by means of a Wien filter to minimise the presence of OH^- species, was employed to sputter secondary ions from the surface of the zircons. Before each analysis, the surface of the analysis site was pre-cleaned by rastering of the primary beam for 3 minutes, in order to reduce the amount of common Pb on the mount surface. The total ion current measured at the mount surface was typically between 1.5 nA and 2 nA, and uniform ion flux across each spot area was achieved by Kohler focusing of the primary beam, which resulted in even, flat-bottomed pits about 1–2 µm deep. Secondary ions were extracted through a low gradient electrostatic field (~4 keV/cm), accelerated to 10 keV, and steered firstly through a double-focusing cylindrical 85° electrostatic analyser with a turning radius of 1.27 m, and secondly through a 72.5° magnet sector with a turning radius of 1 m. Ion currents of the relevant secondary species were then determined by switching the magnetic field to direct the secondary ion beam into a single electron multiplier with a deadtime of 25 ns. Mass resolution (M/ΔM at 1% peak height, as measured on ^{208}Pb on Pb-rich feldspar from Broken Hill) was ~5000, and total Pb^+-ion sensitivity was usually in the range 20–27 cps/ppm/nA.

Data acquisition involved cycling the magnetic field through a run-table comprising the following ten nominal mass-stations and counting times: $^{196}Zr_2O$ (2 s), ^{204}Pb (20 s), background 204.1 (20 s), ^{206}Pb (15 s), ^{207}Pb (40 s), ^{208}Pb (5 s), ^{238}U (5 s), ^{248}ThO (2 s), ^{254}UO (2 s), and $^{270}UO_2$ (2 s). Measurement positions of ^{204}Pb and background at mass 204.1 were fixed relative to the position of $^{196}Zr_2O$, and measurement positions of ^{207}Pb and ^{208}Pb were fixed relative to ^{206}Pb. A full cycle through the mass-stations is termed a scan, and each mass-peak was re-centred once per scan. Each analysis

comprised six sequential scans, and typically took about 24 minutes to complete (including pre-cleaning and beam-tuning time prior to the first scan).

Appendix Table A.1 *Summary of session 130036 metadata, parameters obtained from analyses of $^{238}U/^{206}Pb$ and $^{207}Pb/^{206}Pb$ reference zircons.*

Session:	130036
MountID:	GA6236
Session dates:	8 –13 April 2013
$^{238}U/^{206}Pb$ reference zircon and age:	TEMORA2 (416.8 Ma)
Analyses used:	57 of 57
Slope of robust regression (95% confidence): spot age (Ma) / session duration (hours)	0.063 +0.033/-0.033
Secular drift correction applied:	Yes
Slope of robust regression (95% confidence): $\ln(^{206}Pb^+/^{238}U^+)$ / $\ln(^{254}UO^+/^{238}U^+)$	1.71 +0.22/-0.25
Calibration exponent used (C; equation (3)):	2.00
$^{238}U/^{206}Pb$ session-to-session error (2σ):	0.30%
$^{238}U/^{206}Pb$ spot-to-spot error (2σ):	1.50%
Index isotope for common Pb correction:	^{204}Pb
Mean $^{207}U/^{206}Pb$ date (Ma, 95% confidence):	379 ± 26 Ma
Mean ^{204}Pb overcounts from ^{207}Pb (counts/second, 95% confidence):	0.014 ± 0.013
^{204}Pb overcount correction applied:	Yes
$^{207}Pb/^{206}Pb$ reference zircon and age:	OG1 (3465.4 Ma)
Analyses used:	27 of 27
Mean $^{207}U/^{206}Pb$ date (Ma, 95% confidence):	3466.1 ± 2.3
Mass fractionation correction applied:	No

Analyses were collected in 'round-robin' fashion, with the analytical sequence comprising one measurement from each sample on the mount, in turn. In general, one measurement of a TEMORA2 reference zircon was made after every third or fourth sample analysis, and one measurement of an OG1 reference zircon was made after every second or third TEMORA2 analysis. In this Record, labels for individual zircon analyses (as shown in data tables) take the form X.Y.Z, where X is the 'grain number' (usually assigned sequentially within a sample, at the time of analysis), Y is the 'spot number' within grain X (used to distinguish between spots at different locations within the same grain), and Z is the 'replicate number' within spot Y (used to distinguish between multiple analyses at the same location in the same grain). Nowhere in this Record have multiple analyses been made at the same location in the same grain, so Z is 1 for all analyses.

A.2. Data Reduction and Presentation

Data from the SHRIMP were reduced, calculated and portrayed using Microsoft Excel® 2003, and the add-ins SQUID 2.50.09.08.06 (Ludwig, 2009) and Isoplot 3.71.09.05.23 (May 2009 revision of Ludwig,

2003). The decay constants used are those of Jaffey et al. (1971), together with present-day $^{238}U/^{235}U$ = 137.88, following the recommendations of Steiger and Jäger (1977).

Common-Pb corrections for unknowns were based on measured ^{204}Pb, and a Pb isotopic composition calculated using the single-stage Pb isotopic evolution model of Stacey and Kramers (1975) at a date corresponding to the individually estimated age of each unknown analysis. The result of this calculation is expressed in the data tables, in terms of common ^{206}Pb as a percentage of total measured ^{206}Pb. All isotopic ratios and ages cited in this Record are corrected for common Pb.

Ages derived from the pooling of multiple individual analyses are error-weighted means unless otherwise specified, and their uncertainties are quoted at the 95% confidence level unless otherwise indicated. Each error-weighted mean has an associated Mean Square of Weighted Deviates (MSWD) value, which is a measure of the degree of scatter of the constituent analyses relative to the assigned uncertainties (Ludwig, 2003), and a 'probability of equivalence' (P_{equiv}) value, which is the probability that all of the constituent analyses are equivalent within their uncertainties. By convention, scatter beyond the assigned uncertainties is assumed to be present when P_{equiv} is less than 0.05. In cases where P_{equiv} is equal to or greater than 0.05, but the MSWD value exceeds 1, the implied dispersion of the data-points beyond their analytical uncertainties is acknowledged by expanding the 95% confidence interval of the mean, via multiplication of its 1σ error firstly by Student's t for n - 1 degrees of freedom (where n is the number of constituent analyses), and secondly by the square root of the MSWD value (Ludwig, 2003).

A.2.1. Calibration procedures

Elemental U concentrations in the unknown zircons were calibrated using the M257 reference zircon (840 ppm U; Nasdala et al., 2008), and the power-law relationship proposed by Claoué-Long et al. (1995):

$$\left[{}^{196}Zr_2O^+/{}^{238}U^+\right] = A \times \left[{}^{254}UO^+/{}^{238}U^+\right]^{0.66} \quad (1)$$

where A is a session-dependent constant determined from measurements on M257. All U concentration data tabulated for unknowns have uncertainties of the order of 15–20%, based on the extent of known variations in U abundance in M257.

The values of $^{232}Th/^{238}U$ in the unknown zircons were calculated using the relationship proposed by Williams et al. (1996):

$$^{232}Th/^{238}U = \left[{}^{248}ThO^+/{}^{254}UO^+\right] \times \left\{\left(0.03446 \times \left[{}^{254}UO^+/{}^{238}U^+\right]\right) + 0.868\right\} \quad (2)$$

The values of $^{238}U/^{206}Pb$ in the unknowns were calibrated using the TEMORA2 reference zircon ($^{206}Pb/^{238}U$ = 0.0668, corresponding to an age of 416.8 Ma; Black et al., 2004), and a power-law relationship (Claoué-Long et al., 1995) of the form:

$$\left[{}^{206}Pb^+/{}^{238}U^+\right] = B \times \left[{}^{254}UO^+/{}^{238}U^+\right]^C \quad (3)$$

where B and C are session-dependent constants determined from measurements on TEMORA2. The canonical value of C is 2.00 (Claoué-Long et al., 1995; Williams, 1998), but its session-specific apparent value was determined independently (via calculation of the slope of the robust regression of $\ln[^{206}Pb^{+}/^{238}U^{+}]$ against $\ln[^{254}UO^{+}/^{238}U^{+}]$) in order to inform the decision regarding the most applicable value. In general, the 95% confidence interval of the independently determined value encompassed 2.00, so the canonical value was used.

The values of $^{207}Pb/^{206}Pb$ in the unknowns were monitored using the OG1 reference zircon ($^{207}Pb/^{206}Pb$ = 0.29907 ± 0.00011, corresponding to an age of 3465.4 ± 0.6 Ma; Stern et al., 2009). For each session, the error-weighted mean $^{207}Pb/^{206}Pb$ for OG1 (denoted $[^{207}Pb/^{206}Pb]_{OG1}$) was calculated (Appendix Table A.1), and the procedure of Stern et al. (2009) used to determine an instrumental mass fractionation (IMF) factor (α):

$$\alpha = \left[{}^{207}Pb/{}^{206}Pb\right]_{OG1} / 0.29907 \qquad (4)$$

The session-specific α value is summarised in Appendix Table A.1. In some geological scenarios (e.g. when comparing highly precise weighted mean $^{207}Pb/^{206}Pb$ ages from Archean and Paleoproterozoic rocks), it is desirable to perform session-specific standardisation of $^{207}Pb/^{206}Pb$ and propagate inter-session calibration uncertainties. However, in the samples documented in this Record, zircons of pre-Neoproterozoic age were rarely encountered, and the calculation of weighted mean $^{207}Pb/^{206}Pb$ ages was unnecessary. Uncertainties on individual $^{207}Pb/^{206}Pb$ analyses are governed by (relatively poor) counting statistics, and are almost always large enough that both the instrumental mass fractionation correction and its associated uncertainty are rendered insignificant. Consequently, the tabulated values of $^{207}Pb/^{206}Pb$ for each sample have not been corrected for instrumental mass fractionation.

A.2.2. Propagation of uncertainties

In each session, a 'calibration constant' value is determined for each individual analysis of the $^{238}U/^{206}Pb$ reference zircon TEMORA2 (i.e. $b_i = [^{206}Pb^{+}/^{238}U^{+}]_i/([^{254}UO^{+}/^{238}U^{+}]_i^{C}$). Uncertainties associated with each of these individual 'calibration constants' (i.e. ± b_i) are governed primarily by the counting statistics associated with the constituent isotopic ratio(s). The value of the session 'calibration constant' (B; see equation (3)) is calculated as the error-weighted mean of the session-specific population of individual calibration constants. However, these populations commonly display significant excess scatter, manifested as an MSWD value for B that far exceeds unity, despite the fact that most reference zircons are (by definition) characterised by $^{238}U/^{206}Pb$ homogeneity at a range of scales. This indicates that the values of ± b_i are usually underestimated in going from analysis to analysis. Consequently, SQUID calculates the constant additional uncertainty per spot (expressed as a percentage) that needs to be added in quadrature to each ± b_i value, in order to produce MSWD ~ 1 for the population of b_i values used to calculate B (Ludwig, 2009). This constant additional uncertainty is termed the 'spot-to-spot error' (or 'reproducibility'), and its session-specific 2σ values are presented in Appendix Table A.1. The spot-to-spot error is added in quadrature to the other sources of error (principally related to counting statistics and the common Pb correction) for each value of $^{238}U/^{206}Pb$ in the unknowns, and thus is incorporated in the uncertainties for all individual $^{238}U/^{206}Pb$ values presented in the data tables.

SQUID also calculates an uncertainty for the session-specific calibration constant (i.e. ± B). This uncertainty is termed the 'session-to-session error' (or 'calibration uncertainty'), and its session-

specific 2σ value is presented in Appendix Table A.1. The session-to-session error is not included in the uncertainties for individual $^{238}U/^{206}Pb$ values presented in the data tables, and should be neglected when comparing error-weighted mean $^{238}U/^{206}Pb$ ages for unknowns co-analysed in a single analytical session. However, it must be accounted for when seeking to compare $^{238}U/^{206}Pb$ datasets more widely (e.g. between different analytical sessions), especially when calculating error-weighted mean $^{238}U/^{206}Pb$ ages for unknowns, because the session-to-session error can be of comparable magnitude to the 95% confidence interval arising from population statistics.

A.2.3. Discordance

Discordance is a measure of the internal agreement of the ages derived from the independent $^{207}Pb/^{206}Pb$ and $^{238}U/^{206}Pb$ isotopic systems, within a single analysis. In zircons of Mesoproterozoic and older age, discordance values for single analyses (and discordance patterns within a population of analyses) can provide important information about the timing and extent of radiogenic Pb loss (see Sircombe et al. (2007) and Carson et al. (2010) for more detailed discussion), and are often a valuable indicator of 'geological' data quality. The comparison is less useful in SHRIMP analyses of post-1000 Ma zircons, because the poor counting statistics associated with $^{207}Pb/^{206}Pb$ determinations in these young grains usually result in uncertainties large enough to obscure the 'true' agreement or otherwise of the two isotopic systems. Nevertheless, the comparison has been performed throughout this Record, using the equation:

$$\text{Disc (\%)} = 100 \times \left[\left(^{207}Pb/^{206}Pb \text{ date}\right) - \left(^{238}U/^{206}Pb \text{ date}\right)\right] / \left(^{238}U/^{206}Pb \text{ date}\right) \quad (5)$$

The analysis-specific results of equation (5) are reported in the SHRIMP data tables.

A.3. Session-Specific Calibration and Data Reduction

The data reported herein were obtained over a single analytical session. Calibration characteristics and data reduction parameters for this session are shown in Appendix Table A.1, and described below.

A.3.1. Session 130036: Mount GA6236, 8–13 April 2013

This session encompassed the analysis of six samples:

- MRT R013228 (GA 2152729): Mount Stronach Granite
- MRT R004491 (GA 2152728): Royal George Granite
- MRT R004493 (GA 1951009): Gipps Creek Granite
- MRT R014555 (GA 2152726): Lisle Granodiorite
- MRT R004499 (GA 1950975): The Hazards Granite
- MRT R017895 (GA 2153031): Meredith Granite

The TEMORA2 $^{238}U/^{206}Pb$ reference zircon was analysed during session 130036. Instrument operating conditions did not remain stable throughout the session, with the TEMORA2 dataset showing a trend toward higher $^{238}U/^{206}Pb$ ages as the session progressed (Appendix Figure A.1). The slope of the robust regression of the individual $^{238}U/^{206}Pb$ ages (Ma) against the cumulative duration of the session

at the time of acquisition (measured in hours since commencement) was significantly more positive than zero at the 95% confidence level (Appendix Figure A.1), necessitating the application of a secular drift correction to the $^{238}U/^{206}Pb$ calibration.

The results of independently applying the secular drift correction indicated in Appendix Figure A.1a is shown in Appendix Figure A.1b.

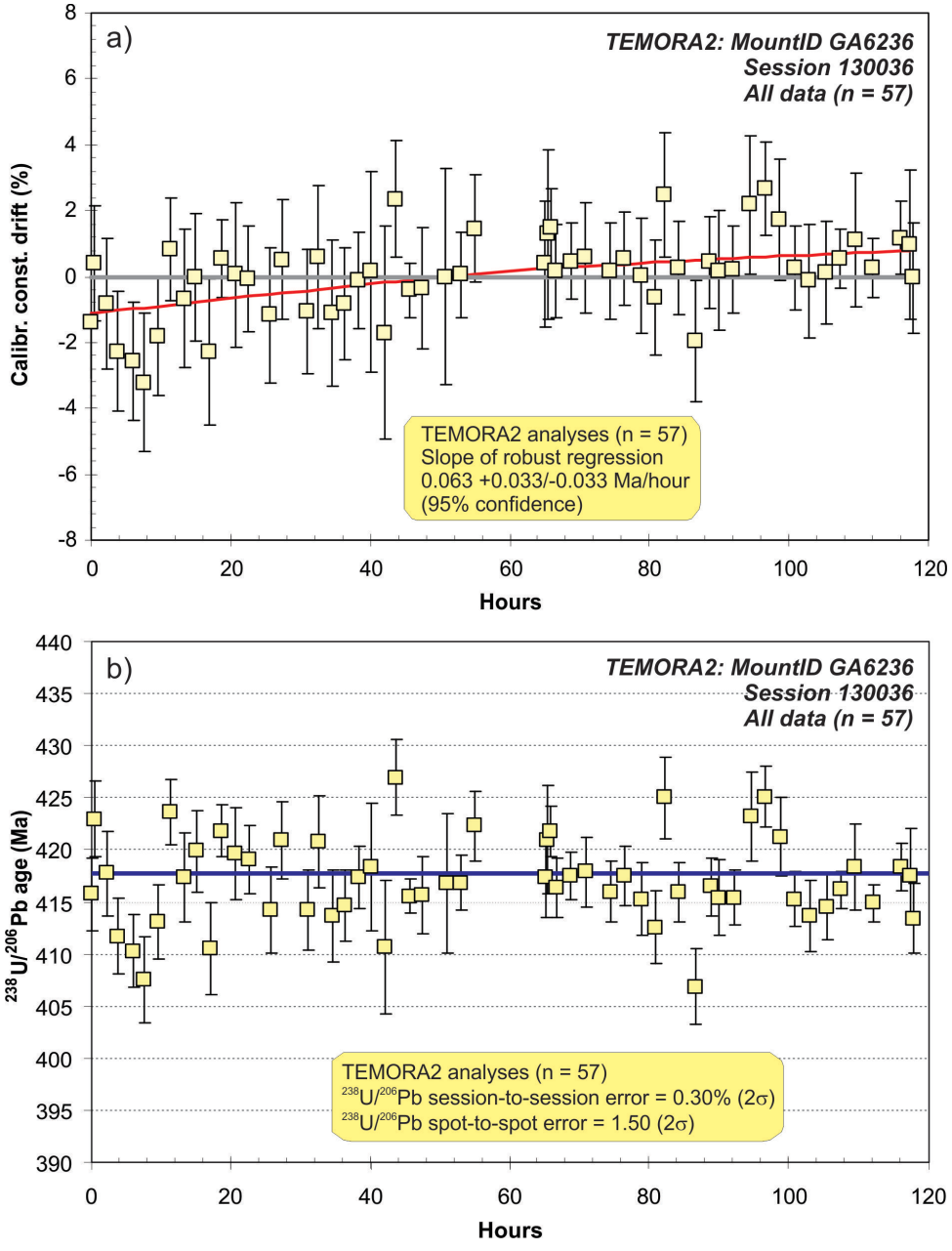

Appendix Figure A.1 *(a) SHRIMP data for $^{238}U/^{206}Pb$ reference zircon TEMORA2 analysed during session 130036, illustrating the existence of measurable drift of the $^{238}U/^{206}Pb$ calibration as the session progressed; Heavy red line - robust regressions of individual $^{238}U/^{206}Pb$ ages against session duration. (b) SHRIMP data for $^{238}U/^{206}Pb$ reference zircon TEMORA2 independently corrected for secular drift. Heavy blue line denotes reference value for TEMORA2 ($^{238}U/^{206}Pb$ age = 416.8 Ma).*

The TEMORA2 dataset displays moderate covariation of ln($^{206}Pb^{+}/^{238}U^{+}$) with ln($^{254}UO^{+}/^{238}U^{+}$), and the slope of the robust regression was relatively shallow (1.71 +0.22/-0.25), but this is primarily an artefact of the secular drift described above, so the canonical value of 2.00 was adopted as the calibration exponent C (see equation (3)). All 57 analyses define a coherent calibration (Appendix Figure A.1b): the weighted mean $^{238}U/^{206}Pb$ value has a session-to-session error of 0.30% (2σ), and a spot-to-spot error of 1.50% (2σ).

The possibility of overcounts at mass ^{204}Pb was monitored by reference to the robust mean of the 57 $^{207}Pb/^{206}Pb$ ages determined for TEMORA2 (379 ± 26 Ma). This result was slightly younger than its reference value (416.8 ± 1.3 Ma; Black et al., 2004) at the 95% confidence level, and raised the possibility that ^{204}Pb was distinguishably 'overcounted' during the session. This idea was supported by estimated ^{204}Pb overcounts based on measured ^{207}Pb (+0.014 ± 0.013 counts per second), and those based on measured ^{208}Pb (+0.029 ± 0.013 counts per second).

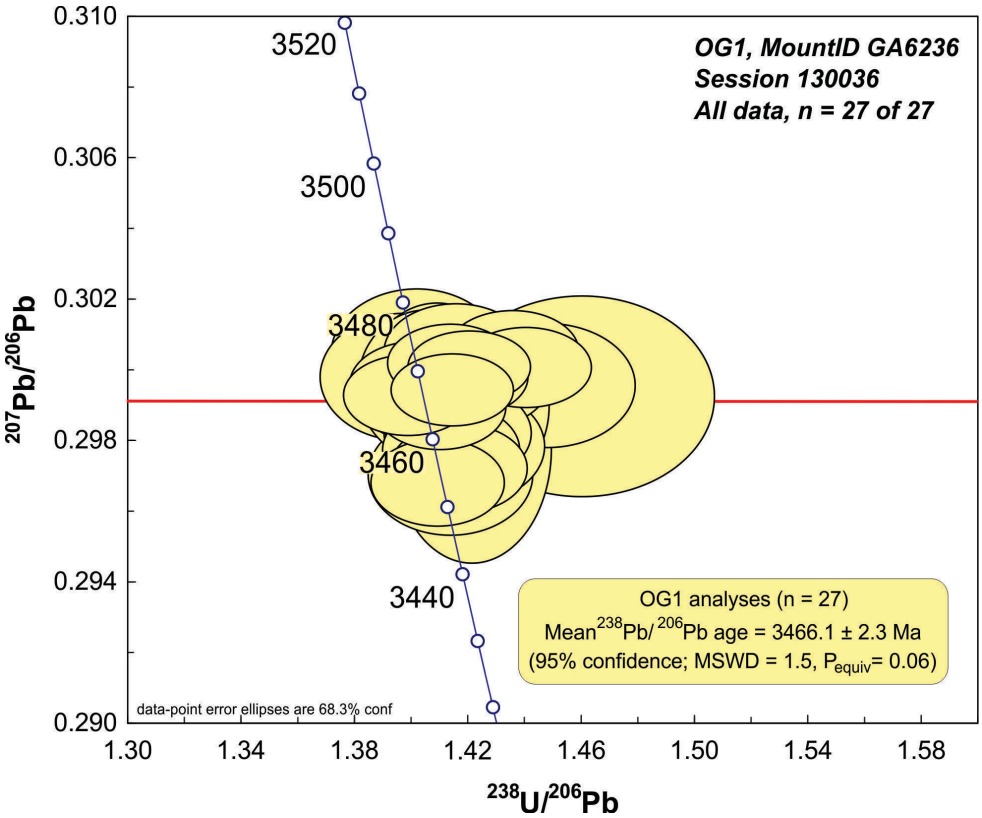

Appendix Figure A.2 *Tera-Wasserburg concordia diagram for OG1 data. Heavy red line denotes reference value for OG1 ($^{207}Pb/^{206}Pb$ = 0.29907).*

In addition, a total of 27 analyses of the $^{207}Pb/^{206}Pb$ reference zircon OG1 were obtained during session 130036 (Appendix Figure A.2). The weighted mean of all 27 $^{207}Pb/^{206}Pb$ ages is 3466.1 ± 2.3 Ma (95% confidence, MSWD = 1.45), and this result is indistinguishable from the OG1 reference value (3465.4 ± 0.6 Ma; Stern et al., 2009), so no correction for instrumental fractionation of $^{207}Pb/^{206}Pb$ was applied.

Machine instability, which led to a period (~8-10 hours) of low beam current (about 50% of normal intensity) within the session, resulted in the loss of 19 analyses. These analyses have been removed from data processing (e.g. Table 3.2 has no analyses numbered 14.1, 15.1 and 16.1).